

Copyright

by

Daniel Edward Wimmer

2017

**The Thesis Committee for Daniel Edward Wimmer
Certifies that this is the approved version of the following thesis:**

**Improved Aerosol Density Sensor for Use in Laser Ablation
of Microparticle Aerosol**

**APPROVED BY
SUPERVISING COMMITTEE:**

Supervisor:

Michael F. Becker, Supervisor

Desiderio Kovar

**Improved Aerosol Density Sensor for Use in Laser Ablation
of Microparticle Aerosol**

by

Daniel Edward Wimmer, A.S; B.S. EE

Thesis

Presented to the Faculty of the Graduate School of

The University of Texas at Austin

in Partial Fulfillment

of the Requirements

for the Degree of

Master of Science in Engineering

The University of Texas at Austin

May 2017

Acknowledgements

I would like to thank all those who have helped and guided me throughout my work to obtain my graduate degree. Foremost, I would like to recognize the dedication and openness of Drs. Michael Becker, Desiderio Kovar, John Keto, and Michael Gammage for their expertise and assistance during the entire extent of this thesis project while welcoming me into their research group, without whom I could not have succeeded. In addition, the detailed design work completed in previous years by Dr. Kristofer Gleason formed the foundation for this project; without his previous sensor development, it would not have been possible for me to finalize this project in the amount of time I had available on campus. The timely endeavors of the UT Physics Department Machine Shop were critical to the mechanical components of the project. My management and technical advisement team at Sandia National Laboratories, Anne Benz and Michael Partridge, helped support and encourage me throughout my academic career at UT. I also extend my appreciation to Jeremiah McCallister for his continued assistance in my understanding of the LAMA system and generously sharing his workspace and time for the testing of my designs. Finally, I would like to thank my wife and sons for their unlimited patience and support throughout my entire academic career.

Abstract

Improved Aerosol Density Sensor for Use in Laser Ablation of Microparticle Aerosol

Daniel Edward Wimmer, M.S.E.

The University of Texas at Austin, 2017

Supervisor: Michael F. Becker

The Laser Ablation of Microparticle Aerosol (LAMA) system in the Nanoparticle Research group at the University of Texas at Austin contains an aerosol density sensor (ADS) component that is critical to achieving accurate results when studying nanoparticle properties. The current ADS at work in the system has been found to possess some data accuracy concerns and a certain lack of usability. To improve on the design, a project was initiated to study the existing sensor to determine the weaknesses of the current design, derive a specific set of requirements for a new sensor, and complete the design and testing of a new ADS for use in the LAMA system. Overall, several major design areas were altered. A completely new LabVIEW data acquisition and processing application was created to monitor, log, and display the density data to the operator, several mechanical components were given additional features to preserve the density signal of the sensor, and the low-voltage DC power supply and signal processing circuitry were significantly redesigned. Advanced testing was performed on the final product to verify that it meets all requirements of the research group and is both reliable and accurate.

Table of Contents

List of Tables	ix
List of Figures	x
Chapter 1: Introduction	1
1.1 Laser Ablation System Overview	2
1.2 Aerosol Density Sensor Overview	3
1.3 Aerosol Density Sensor Objectives	3
1.3.1 Calibration.....	4
1.3.2 Accuracy and Control	5
1.3.3 Data Logging	6
Chapter 2: Sensor Development	7
2.1 Existing Sensor Description.....	8
2.1.1 Existing Hardware	9
Laser Alignment Method	10
Aerosol Flow Box	11
Power Supply	11
Detection and Pre-Amplifier	12
Waveform Generator	14
Lock-In Amplifier	15
Signal Filtering.....	16
2.1.2 Existing Software.....	17
2.2 Development Process.....	18
2.2.1 User Concerns	18
Beam Alignment	18
Inconsistent Sensitivity	19
Calibration Technique.....	19
Power Supply Reliability	20
2.2.2 Hardware Objectives.....	20

Window Gas Flow	20
Apertures	21
Power Supply	21
Sensing and Pre-Amplification	22
Amplification	23
Signal Filtering.....	23
2.2.3 Software Objectives	23
Data Logging	24
Calibration.....	24
Data Display.....	25
Chapter 3: Updated Aerosol Density Sensor	26
3.1 Hardware Description	27
3.1.1 Laser Alignment System.....	27
3.1.2 Power Supply	28
3.1.3 Flow Sensor Box	30
3.1.4 Photodetector and Pre-Amplifier	31
3.1.5 Amplifier	32
3.1.6 Filter	34
3.2 Software Description	35
3.2.1 State Machine Description	36
3.2.2 Calibration.....	37
3.2.3 Data Collection	39
Chapter 4: Test and Experimental Methods.....	41
4.1 Test Setup.....	42
4.1.1 Laser Alignment.....	42
4.1.2 Gas Flow	43
4.1.3 Density Adjustment	43
4.2 Calibration Procedure	44
4.2.1 Algorithm.....	45
4.3 Test Plan.....	50

4.3.1	Lowest Detectable Density	50
4.3.2	Sensitivity Stability	51
4.3.3	Low Density Data Quality	51
4.3.4	Average and High Density Data Quality	52
4.3.5	Run-Time Density Adjustment Response	52
Chapter 5:	Experimental Results	53
5.1	Data Analysis	54
5.1.1	Lowest Detectable Density	54
5.1.2	Sensitivity Stability	56
5.1.3	Low Density Data Quality	58
5.1.4	Average and High Density Data Quality	59
5.1.5	Run-Time Density Adjustment Response	60
5.2	Evaluation of Test Results	61
Chapter 6:	Conclusion.....	63
6.1	Summary of Results	64
6.2	Future Work	64
Appendix A:	Mechanical Drawings.....	66
Appendix B:	Hardware and Circuit Schematics	68
Appendix C:	PCB Schematics	70
Appendix D:	Graphical User Interface Images.....	72
Appendix E:	Software Diagrams	76
References	86
Vita	88

List of Tables

Table 1: Sensitivity Stability due to Window Transmission Data Record	57
---	----

List of Figures

Figure 1. Simplified Block Diagram of Laser Ablation System.....	2
Figure 2: Existing Aerosol Density Sensor Block Diagram	8
Figure 3: Existing Laser Alignment System	10
Figure 4: (Left) X-Y Plane of Existing Aerosol Flow Box; (Right) X-Z Plane of Existing Aerosol Flow Box.....	11
Figure 5: Existing Low-Voltage Battery Pack	12
Figure 6: Sensing and Pre-Amplification Circuitry of Existing Aerosol Density Sensor.....	14
Figure 7: On-Board Function Generator of Existing Aerosol Density Sensor	15
Figure 8: Lock-In Amplification Circuitry of Existing Aerosol Density Sensor...16	
Figure 9: Signal Filter of Existing Aerosol Density Sensor	17
Figure 10: Laser Alignment System of Updated Aerosol Density Sensor	28
Figure 11: Battery Bay Node Diagram	29
Figure 12: Battery Bay Switching Schematic	30
Figure 13: (Left) X-Y Plane of New Aerosol Flow Box; (Right) X-Z Plane of New Aerosol Flow Box	31
Figure 14: Sensing and Pre-Amplification Circuit Schematic of New ADS	32
Figure 15: Lock-In Amplifier Circuit Schematic of New ADS.....	33
Figure 16: Low-Pass Filter of New ADS.....	35
Figure 17: Front Panel of Graphical User Interface of ADS Control Software.....	36
Figure 18: Sample Excel Spreadsheet Exhibiting the Logged Calibration Parameters	39
Figure 19: Front Panel of Exp_Run SubVI in ADS Software Application	40

Figure 20: Sample Excel Spreadsheet Exhibiting the Logged Experiment Data and Operating Parameters	40
Figure 21: Block Diagram of Aerosol Density Adjustment System for New ADS44	
Figure 22: Data Plot of ADS Output in Units of mg/hr for Lowest Possible Density Through the Sensor	55
Figure 23: Zoomed-In Portion of Data Plot of ADS Output in Units of mg/hr for Lowest Possible Density Through Sensor	55
Figure 24: Data Plot of ADS Output in Units of mg/hr for Zero Aerosol Flow through the Sensor	56
Figure 25: 1) Data Plot of ADS Output at 10 Hz representing background and laser scattering offset voltage, V_3 , 2) Data Plot of time-averaged V_3 across several calibrations, 3) Trend of time-averaged values of V_3 across 5-hour interval	58
Figure 26: Data Plot of ADS Output in Units of mg/hr for a Low Density Feed ..	59
Figure 27: Data Plot of ADS Output in Units of mg/hr for a Typical Density Feed	60
Figure 28: Data Plot of ADS Output in Units of mg/hr for a High Density Feed	60
Figure 29: Data Plot of ADS Output in Units of mg/hr During a Run-Time Density Level Adjustment	61

Chapter 1: Introduction

This thesis discusses the flaw analysis, design and implementation of operational improvements to the existing aerosol density sensor (ADS) and its use within the Laser Ablation of Microparticle Aerosol System (LAMA) in the Nanoparticle Research group at the University of Texas at Austin. The circuitry, mechanical drawings, and operation procedures employed in the project heavily reference the work described in the thesis of Dr. Kristofer Gleason [1], who is the designer and creator of the group's original ADS.

1.1 LASER ABLATION SYSTEM OVERVIEW

As illustrated in the block diagram of Figure 1, the laser ablation system consists of several subsystems and individual components. A microparticle aerosol is formed by passing helium through a material powder that typically consists of silver microparticles that are manufactured to have a mean size of around 1.2 μm . These particles are aerosolized inside the powder feeder and then flow through the aerosol flow sensor, where the number of microparticles is continuously measured and recorded in software as a data log. After passing through the density sensor, the aerosol is illuminated by a high-power laser beam. The particles absorb the photon energy and are ablated into much smaller nanoparticles, often with a mean size of around 7 nm. Ultimately, the nanoparticle aerosol travels through a supersonic nozzle and is impacted upon films of varying types of material, forming “samples” of nanoparticle depositions.

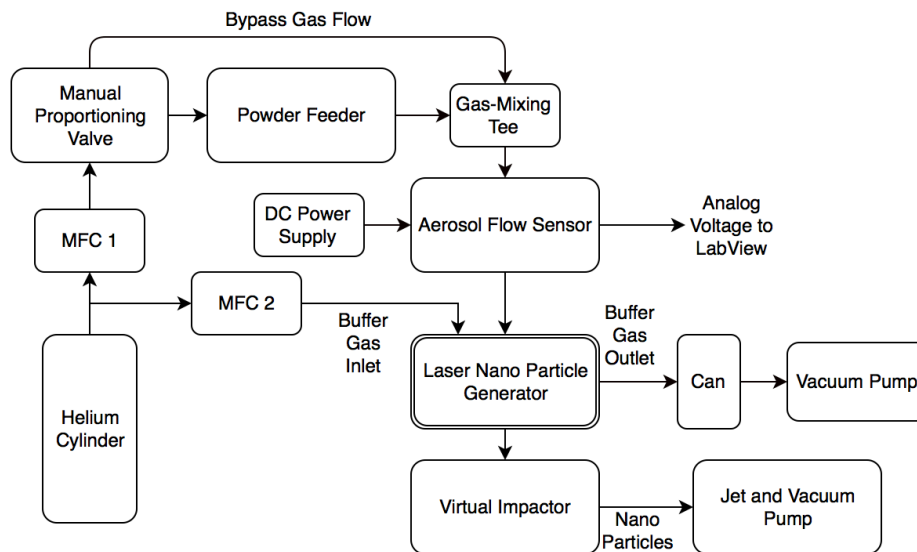


Figure 1. Simplified Block Diagram of Laser Ablation System

These samples are the ultimate product of the LAMA system. The properties of the deposited particles are studied to determine experimentally, along with a parallel study using computer simulations performed at the Texas Advanced Computing Center (TACC), the effect that environment, film orientation and material type, have on the deposition of nanoparticles. Particle properties of differing materials are discovered and used to develop manufacturing techniques for nanocomposite materials and devices [2].

1.2 AEROSOL DENSITY SENSOR OVERVIEW

An aerosol density sensor is used to continuously measure and record the particle number of the aerosol that flows through it in real-time. Using photon scattering of a laser beam that is directed through the aerosol along with low-noise amplification circuitry, a very low-density aerosol can be observed and accurately measured. The pulsed diode laser is incident upon the aerosol flow and the 90° scattered light signal is detected by an avalanche photodiode. The signal then proceeds to low noise, high gain amplification circuits. As part of the signal detection chain, a lock-in amplifier takes the input signal and amplifies those components that are in phase with the laser modulating waveform while minimizing the noise components. In effect, this is a highly selective filter at the pulse frequency of the diode laser. The final output signal from the ADS is digitized and further processed by computer software, logged with respect to time, and displayed to the operator in a graphical user interface (GUI).

1.3 AEROSOL DENSITY SENSOR OBJECTIVES

The aerosol density sensor must be designed such that it satisfies several primary objectives to make it a useful and reliable subsystem of the laser ablation system. The

data resulting from the sensor is used to monitor and control an important parameter of the LAMA samples, which is aerosol density and microparticle number. A reliable calibration process must be featured by the ADS so that the quality of the data between different experiments remains consistent. Since the particle count can be accurately captured and logged throughout the experiment, it allows the operator to make a more knowledgeable study of the films and become more accurate at deducing conclusions from the LAMA results. Without the ability to quantify and control the density, it is impossible to make accurate conclusions about those properties of the resulting films that are dependent upon this parameter. The density levels used by the LAMA system are significantly lower than most typical aerosol processes, which presents a further challenge to the sensor. By displaying the value and trend of the particle count to the operator, necessary adjustments to the density can be made so as to keep the particle number as constant as possible. These requirements must be met in order to consider the data as valid when using it to compare or characterize the nanoparticle deposit films that are produced as the final product of the LAMA.

1.3.1 Calibration

A complete calibration process must be in place to guarantee that data taken from the ADS can be trusted and qualitatively compared across separate experiments. The main goal of the calibration is to convert output voltage to aerosol density in units of milligrams per hour, micrograms per cubic centimeter, and particles per cubic centimeter, while removing the effects that electronic and environmental variables have on the operation of the sensor. Perhaps the most important function of the sensor calibration is the voltage-to-density conversion that is performed in software. Though it is possible to

use mathematical equations such as the Beer-Lambert Law to determine the proportionality constant that should be applied to a measured voltage from the photon collection device circuitry to convert it to density [3], it is much simpler and more accurate to perform an intelligent measurement in software to calculate the conversion. By having knowledge of the mass that has passed through the system, it is possible to determine how the voltage corresponds to a certain unit of aerosol density. In addition, by performing a system calibration at startup or any time a major operating parameter is changed, many non-ideal settings or variation in APD bias voltage will no longer have a significant effect on the normalized data taken at the output of the ADS. Thus, the operator can rely upon the sensor data with much less concern for the inconsistent environment.

1.3.2 Accuracy and Control

It is essential that the design of the ADS ensures an accurate reading of the aerosol density and gives the operator the ability to adjust the settings on the powder feeder as necessary to maintain an approximately constant density level over time. The ADS records the aerosol density over the period of an experiment. For an ideal deposition film, it is desirable to have the aerosol be as consistent as possible across the area of the film. It is important that the operator can be certain of the behavior of the density over the deposition of a particular film so that the actual particle density can be documented so that the quality of each film can be correlated to the aerosol density used to prepare that film. Knowledge of the density also allows the efficiency of the LAMA to be determined; a measurement of the volume of material in the resulting film can be compared to the total mass fed through the system to calculate the efficiency of the deposition process.

1.3.3 Data Logging

The ADS must have a feature that keeps a log of the data taken from the sensor. A file is created that lists aerosol density and particle number data with time stamps that can be directly compared to the time a film was created. The ability to quantify the density, and therefore mass, of the particulate being fed through the system allows researchers to troubleshoot unexpected results on deposition films. Significant fluctuations, especially short peaks, in the density must be captured. Typically, there is a maximum density that can be fed through the system without introducing these agglomerates, which are clumps of particles that become fused together or larger particles that escape being ablated. Bursts of particles from the powder feeder cause peaks in the aerosol density that must be recorded to allow the researcher to recognize that a particular instance of agglomeration has been caused by a simple case of excessive density versus some other systematic problem or unexpected nanoparticle characteristic. Over the course of making several films, the ability to document the density allows it to no longer be considered a mostly unknown parameter. Qualitative analysis of particle behavior can be more accurately examined when the effects of density fluctuations are more accurately known and accounted for.

Chapter 2: Sensor Development

This chapter provides a detailed description of the aerosol density sensor originally designed in a previous dissertation that is currently employed in the LAMA system [1], the general process that was followed while planning and designing the new sensor, and the objectives that were determined to be necessary in the new design. Though several existing attributes and functionalities were changed along with the addition of many new features in the updated version of the ADS, the signal flow process and base mechanical and electronic designs remain largely as described in this section.

2.1 EXISTING SENSOR DESCRIPTION

The design details and circuit schematics of the existing aerosol density sensor are taken from the work documented in the dissertation of Kristofer Gleason [1]. To describe the general operation, the following block diagram should be referenced.

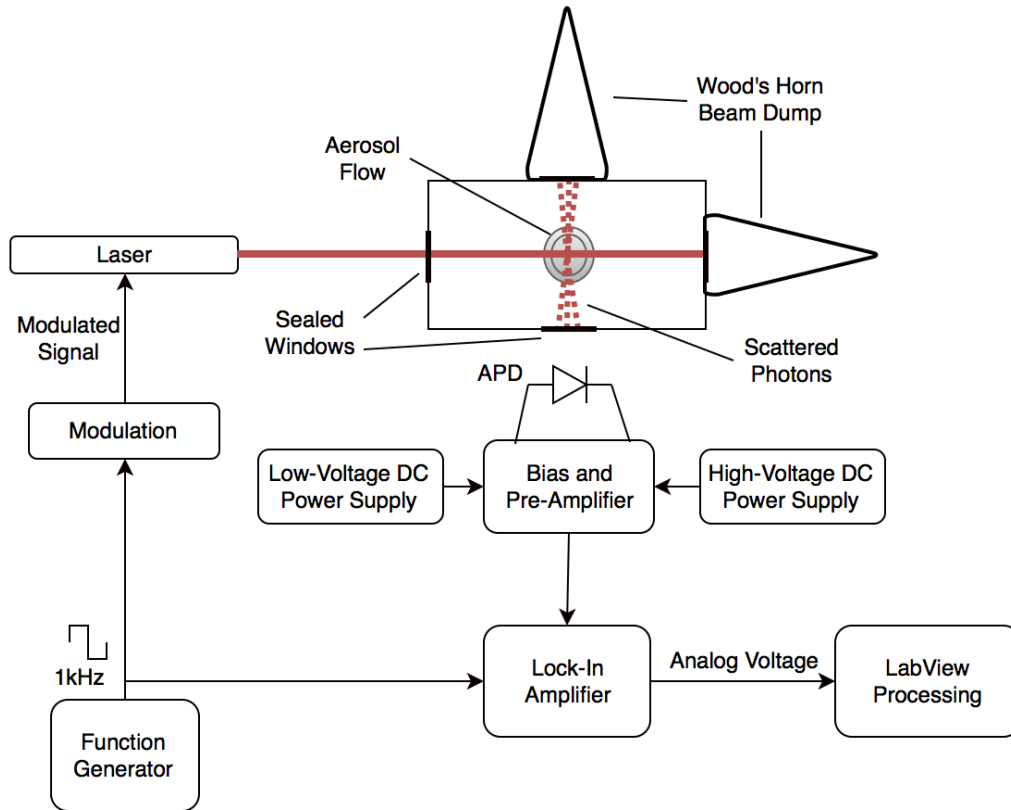


Figure 2: Existing Aerosol Density Sensor Block Diagram

Mechanically, the aerosol flows through two 1/4" diameter stainless steel tubes that extend through the aluminum aerosol flow box and are aligned such that there is a small gap of approximately 1/8" between them in order to expose the flow to the sensing components of the APD without being so large as to significantly affect the flow itself. Using a custom on-board function generator, an approximately 1 kHz square wave

modulation signal is sent to both a low-power 6 mW laser and a lock-in amplifier integrated circuit located inside the amplification module. The modulated laser beam illuminates the aerosol flow thorough the gap and causes a fraction of the photons to impact the microparticles that are present in the aerosol and diffract away from the flow to be captured by an avalanche photo diode (APD). The APD uses internal avalanche electron multiplication in its junction diode structure to amplify the extremely low current generated by photons being incident upon the active area. The resulting current gain of the APD is non-linearly dependent upon the bias voltage placed across the device and is therefore adjustable. The signal from the APD is amplified by a pre-amplifier with gain that is permanently set in hardware, then proceeds to a variable gain amplifier. Following this, the lock-in amplifier uses both the sensed signal and the reference waveform from the function generator to amplify that element of the signal which is mutually in phase, while effectively cancelling out a large portion of the noise in the signal that is not in phase with the modulating signal. Finally, a variable time-constant R-C filter is employed at the end of the circuitry to further reduce noise in the system. LabVIEW software is employed on a local computer to capture the analog signal after processing and performs data logging. A graphical user interface is also available to the operator to control data acquisition and view density data over time. This same software also employs a function to calibrate the APD on startup or anytime on demand.

2.1.1 Existing Hardware

Each subsystem of the aerosol density sensor employs either mechanical components or circuit hardware in some form. Below can be found a detailed description of the hardware employed in each subsystem of the existing version of the ADS.

Laser Alignment Method

The current version of the laser alignment system is simple. A low-power 630 nm laser is mounted on a standard optical mount with two degrees of freedom allowing the laser to be raised or lowered vertically as well as turn horizontally to the left and right as a unit. A focusing lens is mounted, with the same two degrees of freedom, between the laser and the aerosol flow box inlet window directly in the path of the beam; as the beam passes through the lens, it causes the beam to converge so as to focus its intensity directly at the center of the aerosol flow box inside the aerosol flow. It is desirable to have the laser beam be as focused as possible when passing through the aerosol flow so that the maximum number of photons pass into the aerosol, which results in a higher sensitivity of the sensor. The focusing lens must be the appropriate distance from the aerosol flow to cause the minimum beam width to occur at this location.

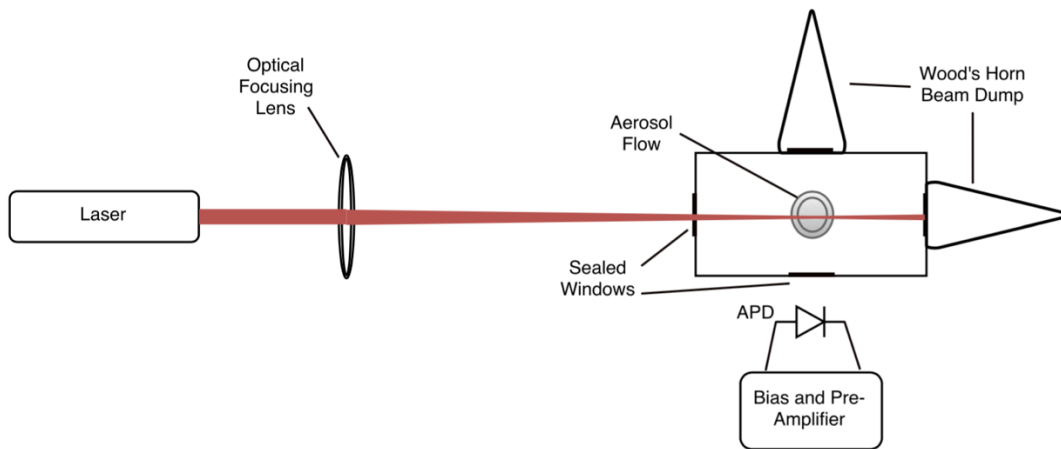


Figure 3: Existing Laser Alignment System

Aerosol Flow Box

The existing aerosol flow box is manufactured out of a solid block of aluminum to reduce the risk of excessive stray light entering it. There are six orifices present in the box, with two along each axis. Along the x-axis, there is a beam entry window on one side and a Wood's Horn beam dump directly across from it to capture the high-intensity laser beam after it passed through the aerosol. A Wood's Horn is a black glass funnel-shaped tube that is used to dissipate any light source that propagates into it. The y-axis consists of a Wood's Horn beam dump directly across from the avalanche photodiode in order to provide a background for the APD that is as dark as possible [1]. Along the z-axis is a stainless steel tube that allows the aerosol to flow into the top of the sensor and exit it through the bottom after passing through a thin gap where it is illuminated by the laser beam.

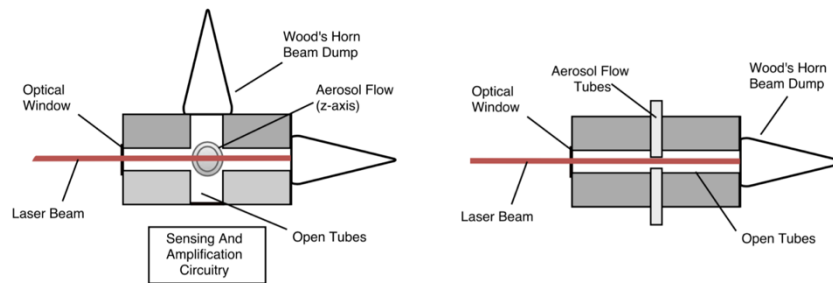


Figure 4: (Left) X-Y Plane of Existing Aerosol Flow Box; (Right) X-Z Plane of Existing Aerosol Flow Box

Power Supply

The power supply for the existing aerosol density sensor consists of two sources: a high-voltage DC supply for APD bias and a low-voltage DC supply for powering the circuitry. The high-voltage supply is taken from a regular laboratory DC power supply

that has the capability of providing up to 260 VDC. The output voltage is adjusted by a rotary knob along with a digital display. The low-voltage supply is taken from two sets of two standard 9-volt alkaline batteries that are forced to have a common ground by connecting the positive terminal of one battery to the negative terminal of the other, effectively providing a ± 9 volt supply. Both the sensing and pre-amplifier circuitry box and the amplification and filtering circuitry box are each equipped with their own battery pack. Batteries were used in the design to provide a steady supply voltage while simultaneously minimizing the noise introduced into the sensor circuitry through the power supply. By using batteries rather than regulating a higher voltage down to the required ± 9 volts, the regulator noise is avoided.

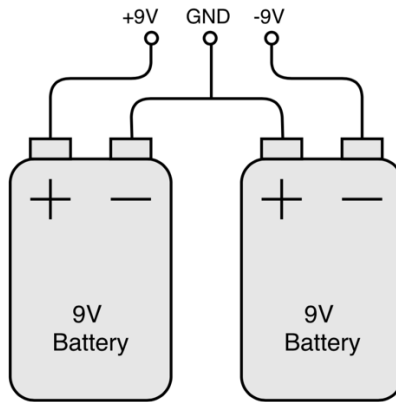


Figure 5: Existing Low-Voltage Battery Pack

Detection and Pre-Amplifier

The hardware in the detection and pre-amplifier module of the existing aerosol density sensor consists of an avalanche photodiode (APD) followed by an amplification circuit. The model of APD used in this design is a Pacific Silicon Sensor AD800, which

has a peak spectral response of 50 A/W at a wavelength of 780 nm, 35 A/W at 630 nm, and a voltage gain of 100 V/V at a bias voltage of 154 volts [4]. The APD's silicon active area, with a diameter of 800 micrometers, is exposed to the aerosol flow through a small aperture in a plate that is mounted to the flow box so as to capture photons that are diffracted from the laser beam as it passes through the aerosol flow and collides with the particles. A small current is generated by the photodiode then amplified using its avalanche electron multiplication property by a multiplier that is directly related to the bias voltage that the APD is exposed to. The APD-generated current is sent through a resistor and the resulting voltage is probed by a balanced pair of instrumentation amplifiers, each with a hardware-defined voltage gain of 501 V/V to an accuracy of $\pm 1\%$. The output of the detection and pre-amplifier module is an analog voltage that has a maximum possible swing of approximately ± 9 volts, though the actual voltage is typically significantly less and is still in need of further amplification. The circuit diagrams for the existing version of the ADS system are taken directly from the dissertation of Kristofer Gleason [1].

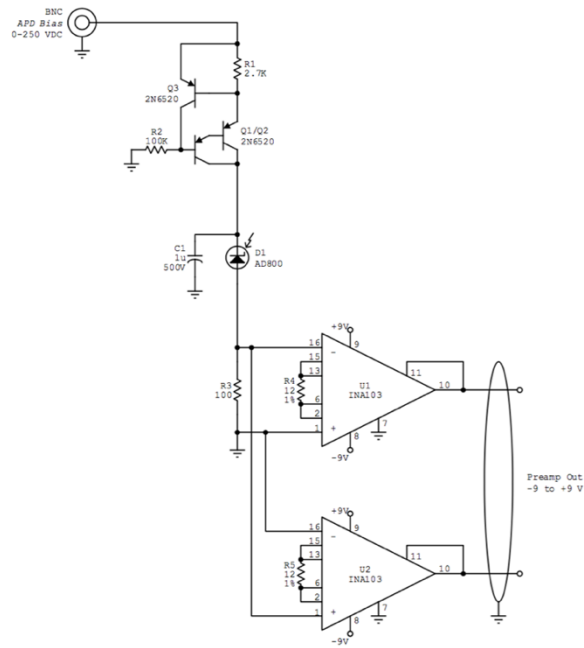


Figure 6: Sensing and Pre-Amplification Circuitry of Existing Aerosol Density Sensor

Waveform Generator

A custom, on-board function generator is present in the existing design for use in both the incident laser and the lock-in amplifier integrated circuit chip. The ± 9 volt battery supply is here regulated down to the 5 volt supply that is necessary for the timer IC present in the waveform generator. Figure 7 demonstrates the general makeup of this feature. An oscillator employs a timer and other passive circuit elements to create a square-wave signal of a frequency close to 1 kHz. This signal is passed to both the laser as the modulating signal for the beam and the lock-in amplifier chip as the reference signal that will be used to amplify those components of the signal corresponding to the aerosol density that are in-phase with the reference.

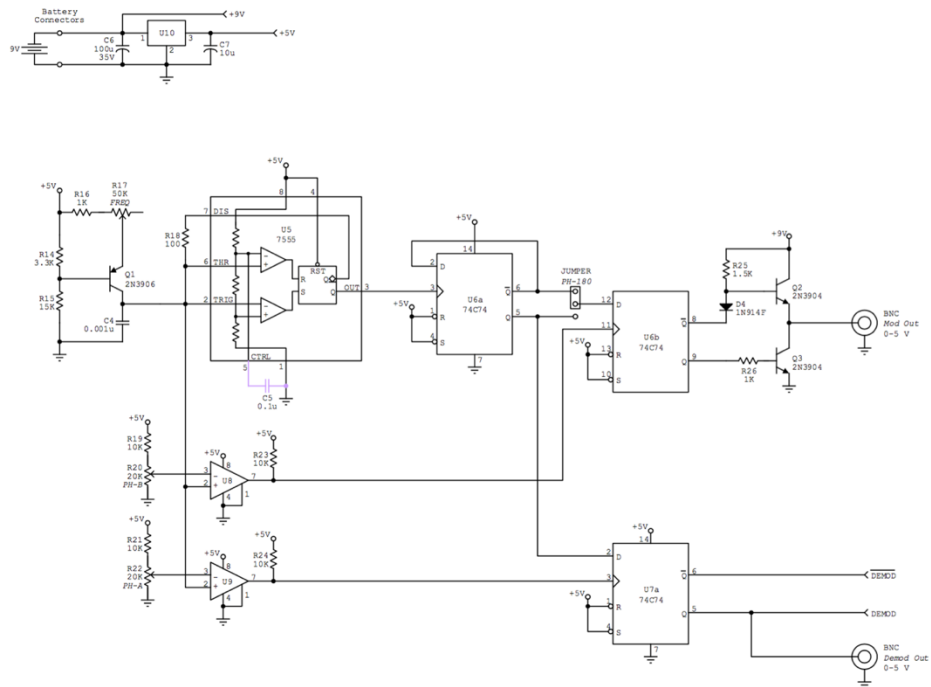


Figure 7: On-Board Function Generator of Existing Aerosol Density Sensor

Lock-In Amplifier

A lock-in amplifier module is employed in the existing design of the aerosol density sensor and is used to amplify the signal components that are in phase with the modulating signal while simultaneously dampening the noise components. The output signal from the sensing and pre-amplification module enters the lock-in amplification module as a differential input and immediately enters an adjustable amplifier that allows the operator to select between an input gain of 1, 10, 100, or 1000. The single-ended output from this stage propagates into a lock-in amplifier integrated circuit that amplifies the signal component that is in-phase with the laser modulation signal. After this stage,

the output signal is again single-ended and contains noise with a lower amplitude than that introduced into the signal by the rest of the laser ablation system.

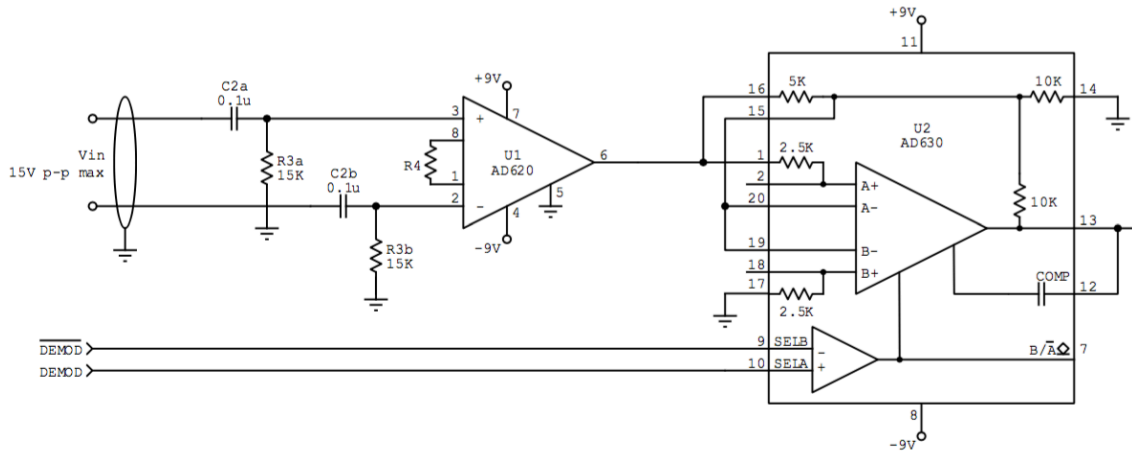


Figure 8: Lock-In Amplification Circuitry of Existing Aerosol Density Sensor

Signal Filtering

The final stage of processing that the density signal is exposed to is the filtering stage. An output amplification stage with an operator adjustable gain of 1 or 10 is followed by a low-pass filter with a permanent time constant of 10 seconds [1]. In addition, this stage is equipped with an offset-adjustment so that the operator can zero the offset present at the sensor output, using both coarse and fine potentiometer adjustment knobs, in order to fully utilize the voltage swing that the sensor is capable of. After this stage, the output signal is monitored in LabVIEW software on a local computer and the voltage is translated into units of density.

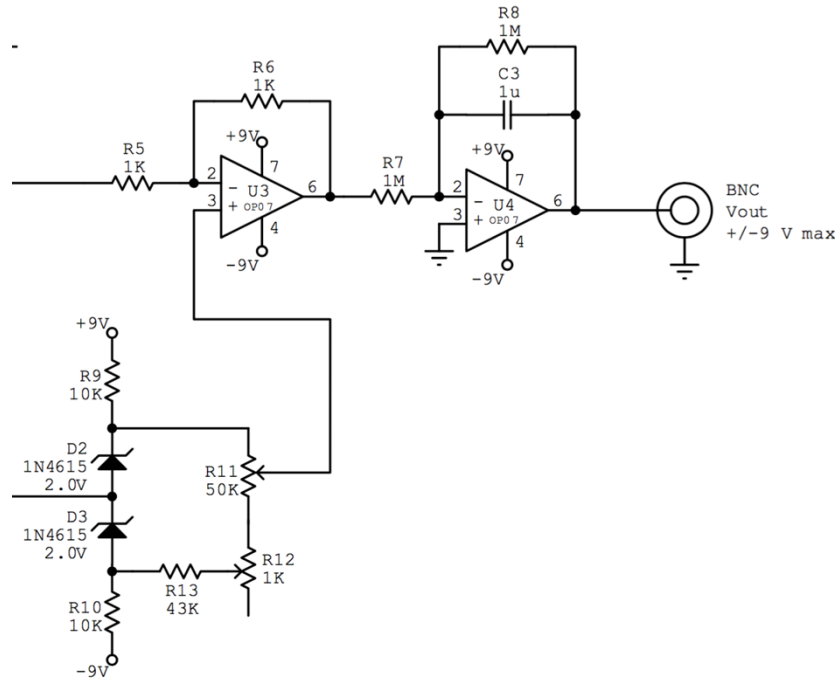


Figure 9: Signal Filter of Existing Aerosol Density Sensor

2.1.2 Existing Software

The software in the existing version of the aerosol density sensor consists of a LabVIEW data logging function. While the sensor is operating, the output voltage node of the sensor is connected to a National Instruments data acquisition unit and monitored continuously. In LabVIEW, the output voltage is saved with its corresponding time stamp every 10 seconds and stored in either a text file or spreadsheet, depending on the preference of the operator, for later use in inspecting particle depositions. A LabVIEW graphical user interface is available for the operator to input offset and voltage average values into a LabVIEW function that will probe the ADS sensor voltage corresponding to density, normalize it with respect to the offsets, and ultimately present it to the operator

as a density measurement in real time. The equation used in this transformation can be found in Chapter 4. The density is displayed in units of particles per cubic centimeter and is written to a spreadsheet file that logs the data for future reference.

2.2 DEVELOPMENT PROCESS

At the start of the research phase of this thesis project, the existing aerosol density sensor was inspected for design inefficiencies and operator-reported difficulties. A concise set of both hardware and software objectives were developed to satisfy the goal of improving the ADS to both make it more effective and more easily used by the research team.

2.2.1 User Concerns

Members of the research team who typically operate the ADS were interviewed in an attempt to pinpoint specific aspects of the sensor that need improvement. The following sections describe the information that resulted from this study.

Beam Alignment

It was found that the current hardware employed for beam alignment was not sufficient. Since the optical mounts for both the laser and the focusing lens each had the same two degrees of freedom, slight adjustment in either resulted in large and mostly inconsistent movement of the laser beam at the window of the flow box. It was difficult to accurately align the laser beam with the aerosol flow using the current setup.

Inconsistent Sensitivity

During experiments that run for longer periods, the sensitivity of the sensor decreased with time. Toward the end of the experiment, the density measurement decreased steadily even if the feed rate was held constant. This inconsistency in sensitivity is unacceptable and one of the most significant problems with the existing sensor, as it causes uncertainty in the overall measurement of the aerosol density, which is the ultimate measurement of the ADS.

Calibration Technique

To perform a calibration on the existing sensor, a Keithley data acquisition unit was programmed to measure the ADS output voltage during several separate system configurations. Using these signals, the background and stray laser beam light levels were measured and the density signal was normalized by accounting for these voltages. After accounting for offset voltages, the sensor was operated for a period of one hour while running a typical aerosol density level. The output voltage was averaged over this time period and the mass of the passed aerosol particulate was measured. The resulting voltage was used to translate instantaneous output voltage into units of aerosol density. Since the user was required to record voltage data from the Keithley data acquisition hardware and manually report it to the LabVIEW software, it was easy for the calibration process to become confusing and inconsistent. This inconsistency can result in inaccuracies in the measured aerosol density reported by the ADS system.

Power Supply Reliability

The low-voltage DC power supply was taken from two sets of dual 9 volt batteries. These batteries continuously drained and it was difficult to determine when they still had power available for operating the sensor, or if they need to be replaced. Not only was this unreliable, but the cost of replacing these batteries multiple times per month became expensive. The inconvenience of not being certain of the state of the batteries or knowing whether the sensor would operate for the full duration of an experiment had caused the system operator to remove the batteries and attach two separate DC power supplies to the test setup in order to provide the necessary ± 9 volt rails. This was not ideal, as the additional power supplies were large and made it difficult to set up the ADS in the laser ablation system due to space constraints and even caused the sensor to occasionally not be used during experiment runs.

2.2.2 Hardware Objectives

Upon studying the design of the existing aerosol density sensor and collecting user data from the system operators, a specific list of hardware objectives was created. In order for the new design of the ADS to be considered a successful project, it is a minimum requirement that all the specified objectives be completed.

Window Gas Flow

It was determined that a major factor affecting the unstable sensitivity of the aerosol density sensor was the presence of an inadvertent collection of aerosol particulate on both the laser beam entry optical window and on the window of the aerosol flow box directly between the aerosol flow and APD sensor. Even as the flow is held constant, the

window steadily becomes more coated with particles and is able to transmit less light. As the APD senses less light, the system falsely responds by measuring that the aerosol density is slowly decreasing.

To counteract this undesirable deposition of particulate, a very low flow of clean gas will be made present at both windows of the flow box, with a direction of flow from the window toward the vertical aerosol flow. Since this newly introduced flow will be of a magnitude of around 5% of the aerosol flow itself, it will not cause any noticeable effect on the flow but will prevent the majority of stray aerosol particles from gradually moving toward and settling onto the windows.

Apertures

Apertures in the tube between the laser beam entry window of the flow box and the aerosol flow will be added to serve a dual purpose. Firstly, the apertures will significantly reduce the amount of background light present in the environment around the ADS that propagates through the flow box to be detected by the APD; as the voltage caused by this light level is decreased, the sensor has a higher swing that can be used to amplify the actual density signal rather than having devoted part of its performance to an offset. Secondly, the apertures will cause a massive decrease in the amount of particulate that can leave the aerosol flow and settle on the window, causing less variation in the sensor sensitivity.

Power Supply

The disposable battery packs of the low-voltage power supply will be replaced with a battery bay of rechargeable 9 volt batteries. Though the rechargeable batteries will

not have an infinite lifetime, they will possess a significantly longer life than disposable batteries and reduce the cost of powering the ADS. A switch will be built into the design so that the operator can quickly and easily transfer the battery bay from operate mode to charge mode after each experiment to guarantee that the power supply will be ready and at full capacity for the next experiment. As previously mentioned, the on-board function generator will be removed from the design and replaced by a node that will be attached via BNC cable to a simple external waveform generator whose output signal is easy to monitor.

Sensing and Pre-Amplification

Several updates will be performed on the sensing and pre-amplification module of the ADS. The current model of avalanche photodiode will be replaced with a different model that possesses both a more desirable response at the wavelength of the diode laser that is being used and a larger active area so that the device is better equipped to provide a high output signal from the sensor under these operating conditions. Also, a JFET operational amplifier will be added to the circuit immediately after the APD to act as a transimpedance amplifier with a very large gain; the main purpose of this addition will be to reduce the Johnson noise of the sensor circuitry [5]. The dual instrumentation amplifiers present in the pre-amplifier will remain in the design but their gain will be reduced dramatically to accommodate the increase in gain from the JFET amplifier that precedes them.

Amplification

As for the amplification module of the ADS circuitry, several changes will be made. The lock-in amplifier present in this circuit will be simplified by removing the on-board function generator and simply adding an input node to the circuit for an external waveform generator. This change will cause the waveform generator to be more easily debugged and verified during operation and will also cause the laser beam modulation signal to be more in-phase with the lock-in amplifier reference signal than it previously was, since the waveform generator will no longer be significantly closer to the lock-in amplifier chip than to the laser beam.

Signal Filtering

At the last stage of the hardware controlled signal processing of the density signal, the low-pass filter currently present in the existing design will be updated in the new design to possess a capacitor bay that allows the operator to easily adjust the time constant of the filter. At least five different time constant settings will be available so as to better record transient peaks in the aerosol flow density. Typically, the sample frequency of the sensor will be around 10 Hz with a R-C filter time constant of 100 ms.

2.2.3 Software Objectives

Similar to the hardware objectives, a concise list of software features that must be incorporated into the new sensor design was created. Since the existing ADS does not possess many GUI or calibration features, it was mandatory that a vast improvement be made.

Data Logging

For the duration that the ADS sensor is running during an experiment, the software will create a data log file that includes both the raw output voltage of the sensor and the corresponding density value along with the appropriate time stamp for the measurement. The frequency at which the data is recorded will be no less than 1 Hz, which is a minimum of 1 sample per second. This increase in the sample rate is necessary to monitor the activity of the aerosol density level to the degree that it can be more closely studied along with the pattern resulting on the particle depositions from the laser ablation system.

Calibration

An automated calibration procedure will be incorporated into the LabVIEW software and will provide the operator with organized and detailed instructions. This feature will cause every calibration of the ADS to be consistent and accurate. Compared with the existing calibration technique, there will be added ease as the LabVIEW software will both provide instructions, acquire the necessary data, calculate a proportionality constant to convert output voltage to units of density, and automatically perform normalization and offset-adjustment as needed. The operator will be able to input the mean particle diameter for the particular feedstock being used in the experiment to allow the software to calculate the number of particles present per cubic centimeter in the aerosol flow; the mean size of the silver feedstock used in the LAMA experiments has been accurately obtained by SEM observations, but the size of other feedstocks is assumed to be accurate as provided by the manufacturer.

Data Display

The new version of the graphical user interface will allow the user to monitor both the past and present activity of the aerosol density level. A plot and numerical display will be presented to the user and will append in real-time with the instantaneous values of voltage and density. The aerosol density will no longer be represented only in units of particles per cubic centimeter, but will also display units of milligrams per cubic centimeter and milligrams per hour, which are independent of the assumed particle diameter of the feedstock and useful to different researchers who rely on varying units of density.

Chapter 3: Updated Aerosol Density Sensor

This chapter is a detailed description of the updated version of the aerosol density sensor that is newly employed into the LAMA system. The design of the new sensor relies heavily upon the foundation laid out in the existing version of the ADS. Many of the hardware features of the existing ADS are still present in the new sensor and continue to be used, though several new features have been added and various designs were altered. Software has been developed that is significantly more advanced than that used for the existing sensor and contains features for calibration, data logging, and density level control.

3.1 HARDWARE DESCRIPTION

Several alterations and additions were made to the existing hardware in the ADS. Both the laser alignment system and low-voltage power supplies were completely redesigned to make each more reliable and manageable to use. The aerosol flow box from the existing sensor has been modified to reduce the amount of particulate that settles on the optical windows to preserve the sensitivity of the ADS. Finally, the sensing and amplification circuits were modified to further reduce electronic noise, while adjustability was added to the filter to allow for more advanced control between the software and hardware of the sensor.

3.1.1 Laser Alignment System

The laser alignment system employed in the updated version of the ADS consists of a total of four optical mounts. A diode laser is placed in a mount possessing two degrees of freedom, horizontal and vertical. Two high-reflectance optical mirrors are placed in mounts capable of tilting both horizontally and vertically by twisting screw knobs; these mirrors can be adjusted very accurately as minute turns on the knobs result in small changes in the beam location at the flow box and there is no need to hold the mount in place while using a tool to tighten it down to its current location. As shown in the figure below, these mirrors are placed in the beam path, between the laser and the focusing lens. The lens is placed at a distance away from the aerosol flow location so as to have the maximum focus of intensity occur inside the flow. In the absence of the aerosol flow box, the laser beam is passed through the focusing lens and the beam size is observed at different distances from the lens. By visual inspection, the distance from the lens that results in the smallest, most focused, beam diameter is documented. Finally, the aerosol flow box is mounted with its center located at this distance from the lens.

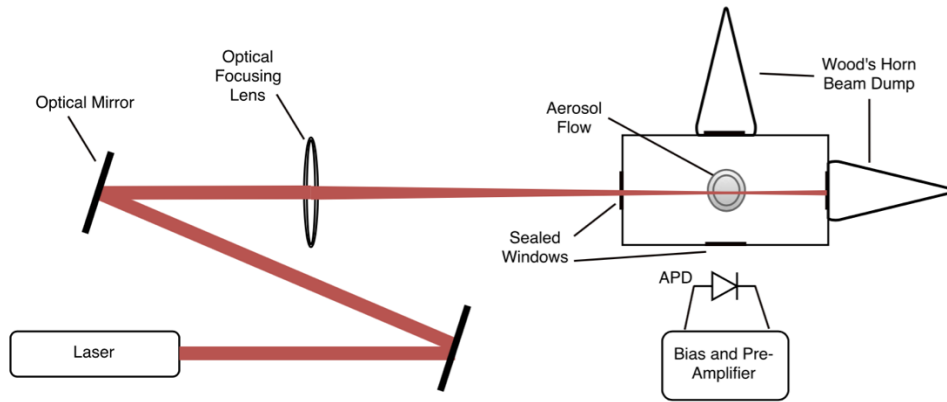


Figure 10: Laser Alignment System of Updated Aerosol Density Sensor

3.1.2 Power Supply

In the new sensor design, power supplies have been updated to improve reliability and simplicity of design. The on-board waveform generator has been replaced with an external function generator that provides a consistent and verifiable square wave modulation signal to the diode laser and internal lock-in amplifier. Though the bias DC voltage supply was not exchanged for a different method of providing high voltage, the operating bias voltage has been reduced from 155 volts to 145 volts, due to the fact that the new sensing circuitry provides a higher hardware gain which allows for the demand on the APD amplification circuitry to decrease. This reduction in bias voltage to the APD from that used in the existing sensor improves the stability of the signal, since the APD gain is exponentially higher at high bias and the signal is significantly more affected by minute variations in bias voltage when operating at higher gain. Finally, the two sets of dual alkaline batteries have been replaced with a battery bay that consists of ten Tenergy 200 mAh NiMH rechargeable batteries which provides a ± 9 volt supply. This battery bay is equipped with a toggle switch that allows the operator to quickly change the operation

mode between discharge and recharge; upon completion of an experiment, the toggle switch can be used to instantly connect the batteries to a 10-channel smart battery charger with built-in capacity monitor hardware that causes the charger to automatically stop charging once it is determined each battery is at full capacity [6]. All switches in the circuit simultaneously switch together when the exterior toggle is operated. The schematic of the battery bay can be found in the images below.

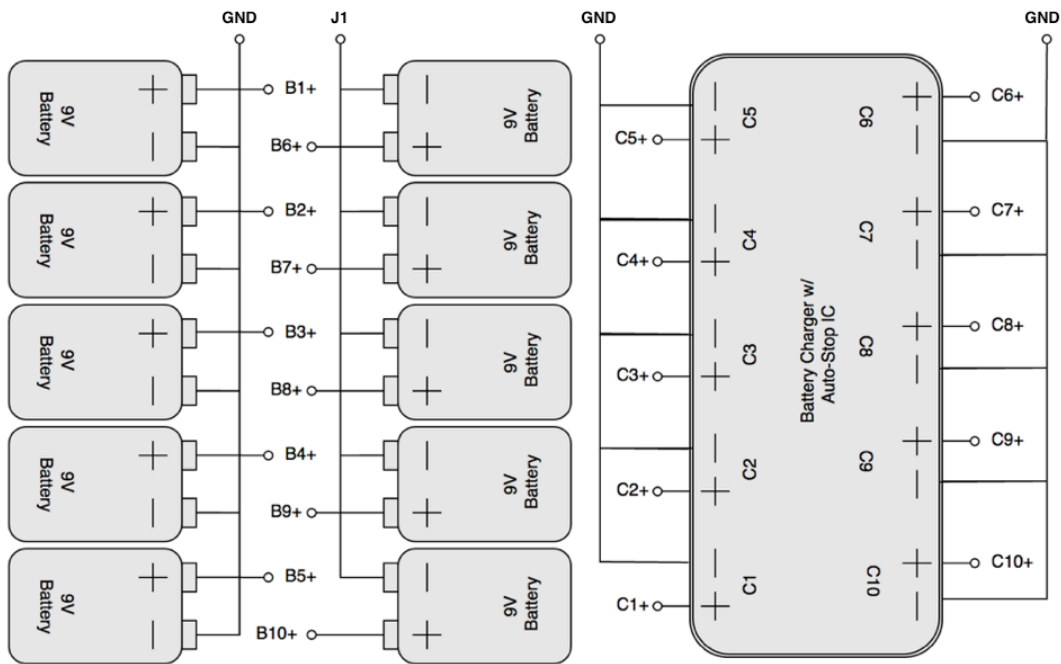


Figure 11: Battery Bay Node Diagram

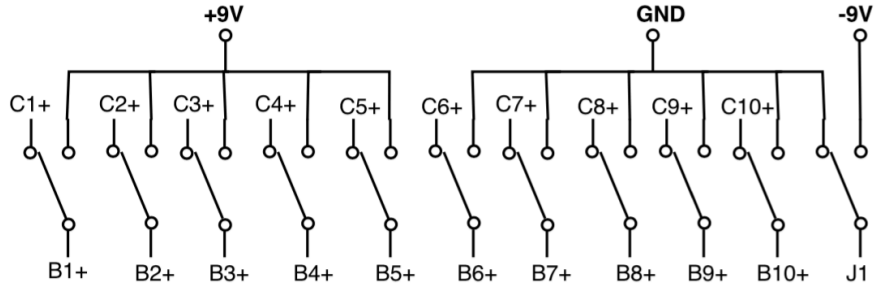


Figure 12: Battery Bay Switching Schematic

3.1.3 Flow Sensor Box

The flow sensor box in the updated version of the ADS is identical to that used in the previous version aside from two added features. Firstly, two thin apertures were punched out of sheet aluminum and installed with even spacing in a thin-walled copper tube that is inserted into the aerosol flow box in the cylindrical cavity between the laser beam entry window and the aerosol flow. Circular holes were drilled in each aperture of diameter 0.08", which is slightly larger than the beam width; this allows the laser beam to travel through the tube unobstructed while simultaneously minimizing the amount of stray light that passes from the exterior environment and into the flow chamber to be detected by the APD. Secondly, the flow box is machined with an inlet tube that allows a low flow of cleansing gas to enter the tubes inside the box and flow with a direction from both optical windows toward the aerosol flow. This gas flow prevents stray particulate from travelling to and settling upon the optical windows and causing variation in the sensitivity of the sensor. Since this flow is limited to 5% of the aerosol flow, it has no significant effect on the flow itself.

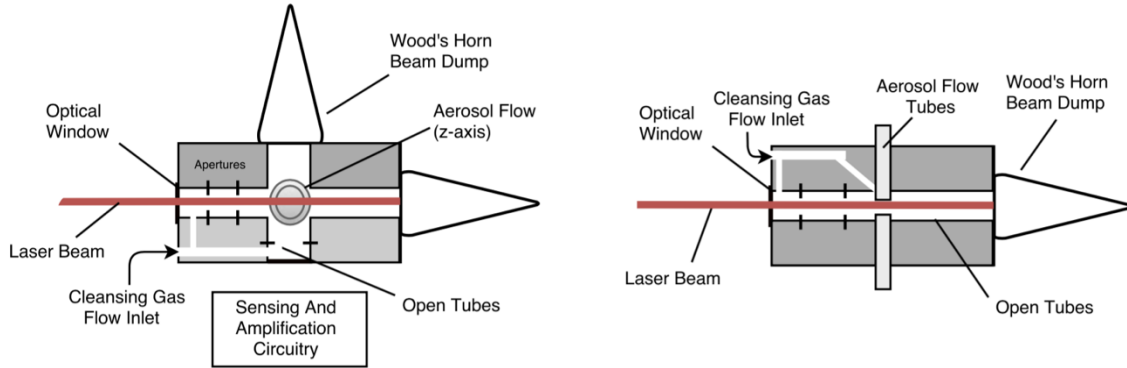


Figure 13: (Left) X-Y Plane of New Aerosol Flow Box; (Right) X-Z Plane of New Aerosol Flow Box

3.1.4 Photodetector and Pre-Amplifier

The photodetector and pre-amplification module of the new ADS has undergone significant changes to its circuitry. The existing model of avalanche photodiode has been replaced with a Hamamatsu S12053-10, which has a peak spectral response of 25 A/W at a wavelength of 620 nm, and a voltage gain of 100 V/V at a bias voltage of 153 volts [7]. Since the active area of this device is 1 mm in diameter, more scattered light will be incident upon it than the previous APD at any given time, resulting in a higher effective sensitivity of the sensor. In addition, a low-noise JFET LT1055 transimpedance operational amplifier has been added immediately after the photo detection circuit with a gain of 200,000 V/A to provide high initial amplification of the signal while minimally increasing electronic noise [8]. Since the majority of the pre-amplification gain is now present in the JFET amplifier, the gain of each instrumentation amplifier was reduced to 1 by leaving the external gain adjustment nodes open circuited. The purpose of preserving the instrumentation amplifiers in the circuit is to provide the following stage of amplification with an optimal balanced differential input while removing most of the common mode component of the signal.

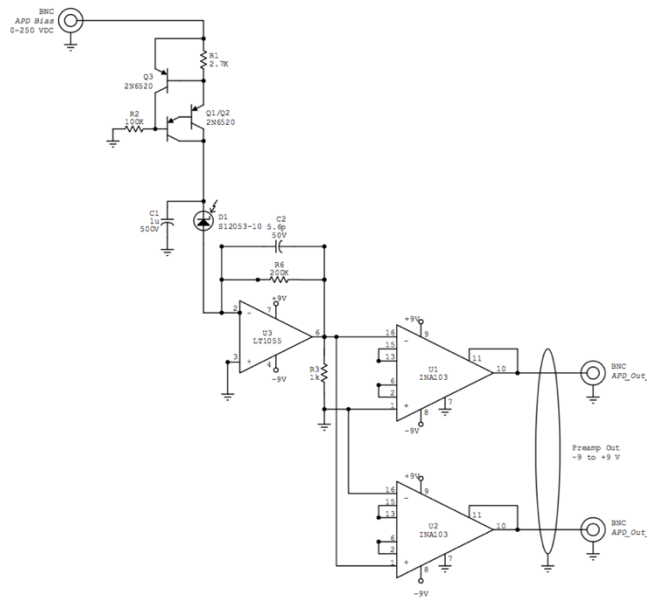


Figure 14: Sensing and Pre-Amplification Circuit Schematic of New ADS

3.1.5 Amplifier

An amplification stage follows the sensing and pre-amplification circuitry in the ADS hardware. The differential input is taken from the output of the pre-amplifier and amplified by a variable gain AD620 instrumentation amplifier. A resistor external to the AD620 is used, along with a rotary switch, to allow the gain of this stage to be set to 1, 10, 100, or 1000 by using Equation 1, where R_4 is the resistor selected by the user via the switch [9]. The ability to vary the gain is useful when performing experiments with different aerosol flow rates. A high flow rate will require less amplification than a low flow rate; this adjustment control prevents saturation of the signal at the supply voltage rails of the amplification circuitry that could occur if the gain of the amplifier is too high with respect to the density signal.

$$Gain = 1 + \frac{49.4k}{R4} \quad (1)$$

Following the amplifier is a lock-in amplifier integrated circuit chip, Analog Devices model AD630. The signal along with the reference waveform generated by the function generator are sent into the IC, where the lock-in amplifier acts as a narrow band filter of a width of approximately 10 Hz that amplifies those components of the density signal that are in-phase with the reference waveform by a gain of 2 V/V while all other noise components are attenuated [10]. The general design of the lock-in amplifier circuit configuration was taken from the work of Sengupta, Farnham, and Whitten as described in Nebraska Wesleyan University's Journal of Chemical Education [11]. A jumper and BNC connection has been added to the amplifier electronics box that allows the user to disconnect the on-board lock-in amplifier from the signal path in order to insert an external full-scale lock-in amplifier if desired. The final output of the amplifier is a single-ended analog voltage signal referenced to ground with a maximum swing of ± 9 volts.

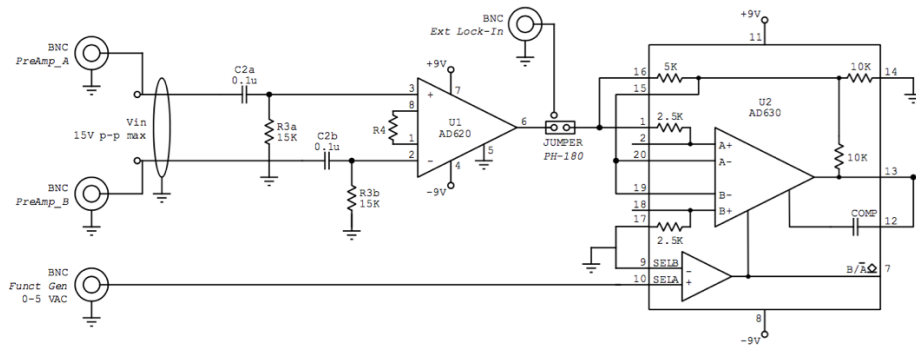


Figure 15: Lock-In Amplifier Circuit Schematic of New ADS

3.1.6 Filter

A low-pass filter and further output amplification circuit follow the lock-in amplifier and high-gain amplification circuitry. The first OP07 operational amplifier employed in the circuit is a unity gain buffer. Along with the offset adjustment resistors, diodes, and potentiometers that are connected to one of its inputs, this module allows the user to adjust two potentiometer knobs, one each for coarse and fine setting, to approximately zero the output voltage caused by electronic noise and DC offsets once the sensor is powered on but not yet calibrated. Minimizing the DC offset at the output of the sensor allows the circuitry to take advantage of the full analog swing that is available to the density signal and avoid clipping or saturation when operating at high gain levels. Lastly, a second OP07 operational amplifier is used as a low pass filter with both an adjustable output gain and R-C time constant, τ . By using Equations 2 and 3, a resistor and capacitor bay is installed to allow the user to use a toggle switch to move between output gains of 1 or 10 and a rotary switch to select between a time constant of 0.01, 0.03, 0.1, 0.3, or 1 seconds. Similarly to the lock-in amplifier, a jumper and BNC connector was installed to allow the user to employ an external lock-in amplifier then re-insert the signal at the input of the filtering stage.

$$|Output\ Gain| = 1e6/R7 \quad (2)$$

$$\tau = 1e6 * C3 \quad (3)$$

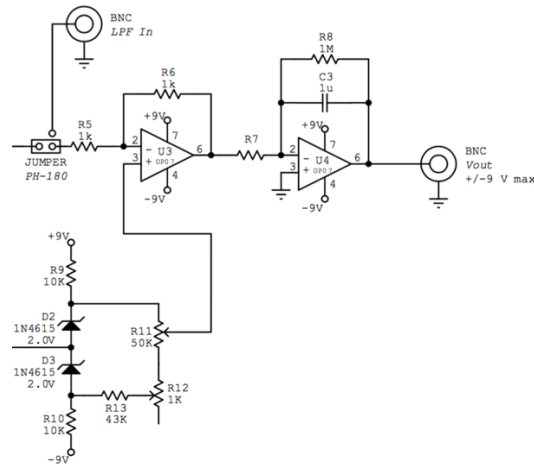


Figure 16: Low-Pass Filter of New ADS

3.2 SOFTWARE DESCRIPTION

The software for the new aerosol density sensor is designed exclusively in the LabVIEW environment. It is generally set up as a state machine that allows the user to run the application and periodically select between different functions, depending on what is necessary at the time of the experiment. A calibration function is integrated into the software that includes detailed instructions to the operator for ease and accuracy of results. The output voltage from the ADS is digitized by a National Instruments myDAQ data acquisition unit and propagated to the LabVIEW application to be processed for unit conversion, data display, and logging with respect to time. All necessary parameters are requested by the program and entered by the user for use in internal calculations and conversions.

3.2.1 State Machine Description

The ADS software application is modeled as a state machine that continuously runs in the background awaiting operator instructions [12]. After pressing the run button in the typical LabVIEW graphical user interface (GUI), the ADS application initializes and takes no further action until it receives a command from the user. As can be seen in the image below of the front panel view of the GUI, the user can select between performing a system calibration, taking experiment data, or exiting the application altogether. The state machine has the property such that after a calibration is performed, the software will continue running and retain the necessary values and calculations to be used in the following experiments.

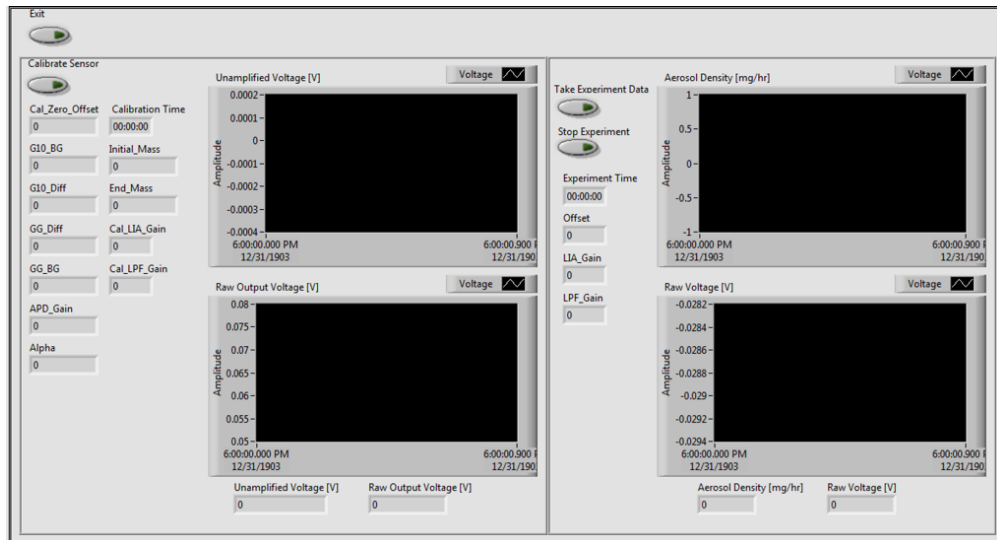


Figure 17: Front Panel of Graphical User Interface of ADS Control Software

3.2.2 Calibration

The calibration function of the ADS software application follows the detailed calibration procedure as outlined in Chapter 4. By setting up the sensor in several different configurations as prompted by the GUI, important information about environment, stray beam scattering, APD gain, and α , the overall proportionality constant used to convert output voltage to units of density, is obtained. During the 30-minute calibration run, the operator can monitor both the raw output voltage and the unamplified voltage that has been normalized by dividing out all gain settings that are adjustable via a visual plot and a numerical display. Using the history of the data on the plot, the operator can judge when an alteration to the density level is necessary and adjust accordingly. All parameters calculated during the calibration function, along with the raw data collected from the sensor, are logged into a .xls spreadsheet file for recording and further processing at a later time, as shown below in Figure 18. The software-calculated parameters are defined as follows:

1. Cal_Zero_Offset is the time-average of the raw output voltage of the sensor over a period of 60 seconds. During this time, the sensor is powered on, the output voltage is manually adjusted to be close to zero using the offset rotary knobs, and no aerosol flow is passing through the system while the laser beam is off. Both variable gain settings must be selected before measuring the DC offset of the sensor, as changes in the gain selection resistors will impact the offset.
2. G10_BG is the time-averaged voltage resulting from background light detected from the environment while the bias voltage is set to provide an APD gain of 10 as defined in its datasheet while the laser beam is off while

gathering data for a period of 60 seconds. The voltage is normalized by dividing the output voltage by the value of all gain settings that are adjustable.

3. G10_Diff is the time-averaged voltage resulting from the combination of both the background light and stray laser beam scattering that is detected by the APD while still operating at a gain of 10 and the laser beam is turned on for a period of 60 seconds. As with the previous variable, the voltage is normalized against the adjustable gain settings.
4. GG_BG is the time-averaged voltage resulting from background light detected from the environment while the bias voltage is set to provide a gain that is temporarily unknown, G, for a period of 60 seconds. The data sheet for the device is used to provide the operator with a guide to approximate what bias voltage should be used to obtain a range of gain values. This value is also normalized to the adjustable gain settings.
5. GG_Diff is the time-averaged voltage arising from the same environmental and stray laser beam scattering as in G10_Diff, while operating at the same bias voltage as that used to obtain GG_10 for a period of 60 seconds. Similarly, this voltage is normalized to the adjustable gain settings.
6. APG_Gain is calculated using the above measured values as defined in the calibration procedure outlined in Chapter 4. This is the internal current gain provided by the avalanche photodiode.
7. Alpha is the overall proportionality constant arising from a completed calibration run. It is used by the software during an experiment to convert the output voltage measured from the ADS from units of voltage to that of density.

	A	B	C	D	E	F	G	H	I
1	Time	Voltage	Unamplified_Voltage [uV]	APG_Gain	G10_BG [uV]	G10_Diff [uV]	GG_BG [uV]	GG_Diff [uV]	Cal_Zero_Offset [mV]
2									

Figure 18: Sample Excel Spreadsheet Exhibiting the Logged Calibration Parameters

3.2.3 Data Collection

After the calibration procedure has been completed, the operator can use the ADS to monitor the aerosol density during an experiment. By selecting “Take Experiment Data”, the application will monitor the output voltage of the sensor at a rate of 10 samples per second and perform the calculations to convert it to the appropriate units of aerosol density. On the front panel of the program, two plots are present along with numerical displays that present the raw output voltage and density data in units of volts and milligrams per hour, respectively. On the front panel of the Exp_Run subVI, the operator can monitor the density in units of milligrams per hour as well as micrograms per cubic centimeter and microparticles per cubic centimeter using real-time plots and numerical displays. When the user presses the “Stop Experiment” button, the software stops collecting data from the sensor and writes the voltage and density data into a .xls spreadsheet file along with the appropriate time stamp for each data point. A sample of the values written to the file can be found in the image below.

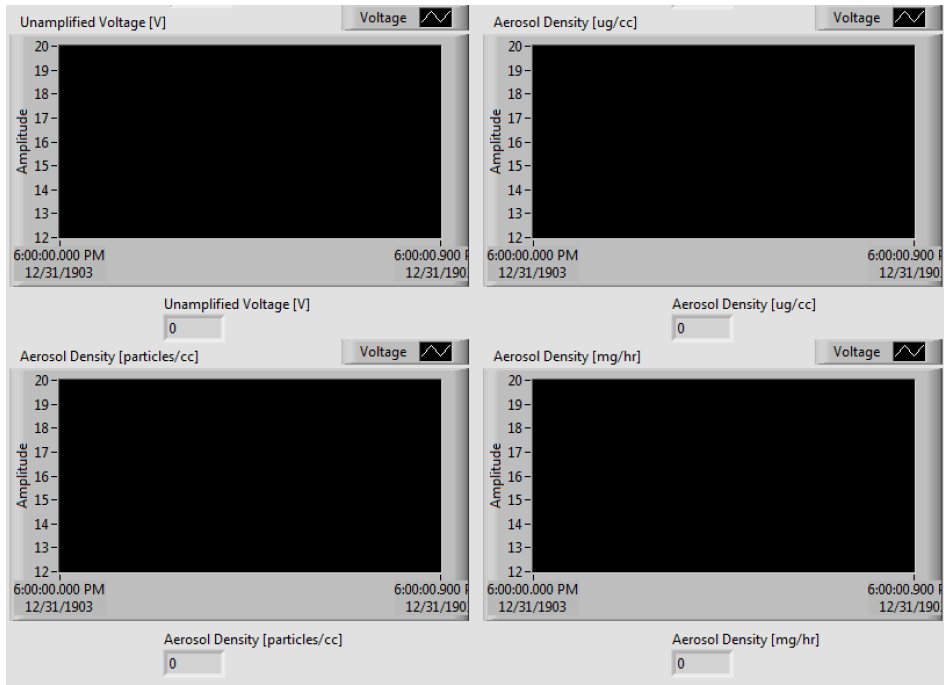


Figure 19: Front Panel of Exp_Run SubVI in ADS Software Application

	A	B	C	D	E	F	G	H	I	J	K
1	Time	Voltage	Raw Output	Raw - Offset	Unamplified [uV]	Density [ug/cc]	Density [particles/cc]	Density [mg/hr]	Alpha	LIA_Gain	LPF_Gain

Figure 20: Sample Excel Spreadsheet Exhibiting the Logged Experiment Data and Operating Parameters

Chapter 4: Test and Experimental Methods

This chapter provides a detailed description of the test setup, calibration procedure, and test plan developed for the new ADS system. Instructions for setting up all necessary components to provide full functionality of the system is included, and can be considered the approach taken for configuration of the test bench used for initial testing of the new version of the ADS. Though the calibration is performed almost entirely in the LabVIEW application, the flow inside the program follows the procedure outlined in this section. Upon completion of the design of the sensor, a test plan was developed as a method of confirming the success of the project, and these critical functionality points are tested as outlined below.

4.1 TEST SETUP

The ADS must be placed in the system such that the aerosol flows vertically through the flow box from the top to the bottom so as to allow the aerosol to flow as consistently as possible with the assistance of gravity. To power on the sensor, the dual toggle switch on the battery bay containment box must be switched to the 'operate' position and the on/off toggle switch on the lock-in amplifier circuit electronics box must be turned to 'on'. The external function generator and high-voltage DC power supply must both be powered on; the waveform generator should be set such that the output is a square wave with a frequency of approximately 1 kHz travelling to the laser and lock-in amplifier. Both the lock-in amplifier and low-pass filter gains should be initially set to 100 and 1, respectively, for the upcoming calibration. The DC offset voltage present at the output of the sensor should be adjusted to be as close to zero as possible via the coarse and fine offset adjustment knobs present on the outside of the amplifier circuit box. Finally, the NI myDAQ unit should be connected to the processing computer that will be used during the experiments.

4.1.1 Laser Alignment

To align the laser beam, the Wood's Horn directly in the path of the beam is removed from the aerosol flow box while the laser is powered on. A piece of white paper is held or mounted where the Wood's Horn is now absent and the beam size is monitored. While independently adjusting both the laser and the focusing lens along the horizontal and vertical axes of their respectful mounts, the beam is observed until it is determined that small movements in the mounts do not result in any significant change in the beam transmittance through the flow box. At this point, it can be assumed that the beam is sufficiently centered within the area where the aerosol will flow and is not excessively

contacting other components inside the flow box. With the laser now aligned, the Wood's Horn is replaced onto the flow box unit.

4.1.2 Gas Flow

Upon startup of either a calibration or experiment run, the ADS LabVIEW application will prompt the operator to initiate an aerosol flow through the sensor at a specified time. The appropriate flow of aerosol through the sensor is 200 cubic centimeters per minute, or 0.2 liters per minute, of helium. This flow is controlled upstream in the LAMA system via a calibrated mass flow controller (MFC) operating at a pressure of 1 atmosphere, and the operator need only turn on the valve at the beginning of the system to allow the flow to pass. Additionally, for the duration that the sensor is powered on, a gas flow of either nitrogen or helium should be set to flow into the cleansing gas inlet tube on the aerosol flow box at a flow magnitude of 8 cubic centimeters per minute using the Omega rotary flow meter present in the ADS system upstream of the MFC.

4.1.3 Density Adjustment

The density of the aerosol in the helium flow is adjusted by moving a manual rotary proportioning valve that determines what proportion of the 200 sccm helium flow is allowed to pass through an aerosol powder feeder, and how much flows as a bypass gas. Typically, a larger flow through the feeder will result in higher densities. By opening the proportioning valve completely, the amount of flow going to the feeder will equal that flowing through the gas bypass, resulting in a minimum flow of approximately 100 sccm through the powder feeder. This configuration is currently not used, because at such low

flow the feeder typically does not consistently aerosolize the particles as there is not enough flow to lift the particles out of the powder and into the rest of the LAMA system. After the powder feeder, the aerosolized flow mixes with the bypass flow in a long glass tube that forms a vortex that is efficient at mixing the particulate evenly throughout the gas, then flows through the ADS to be observed and measured.

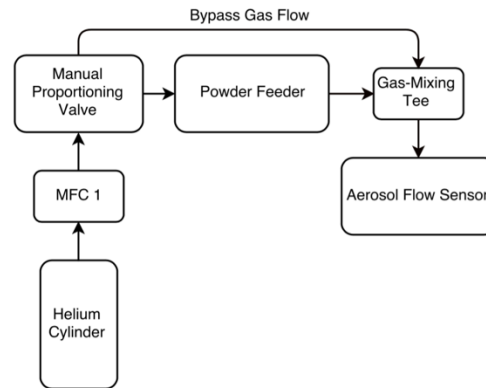


Figure 21: Block Diagram of Aerosol Density Adjustment System for New ADS

4.2 CALIBRATION PROCEDURE

The general form of the calibration procedure for the ADS is referenced from the original design from the Gleason dissertation [1]. Essentially, the ADS is operated in several different configurations in order to capture information about background light, scattered laser beam light, and electronic noise in the sensing circuitry. Using the results of the calibration, the LabVIEW software is able to accurately convert the output voltage of the sensor into useful density measurements while also normalizing the data taken while running an experiment with respect to the DC offset of the sensor and other offset voltages caused by secondary light sources being detected and amplified. A calibration

routine must be performed every time the ADS is powered on, the bias voltage is changed, or the alignment of the incident laser beam is adjusted. This allows for data that is confidently accurate, since small variations in the configuration of the sensor will change the proportionality constant that is used almost exclusively to convert voltage to units of density. Using the values calculated during the calibration, the LabVIEW program is able to provide the user with the instantaneous aerosol density in units of mg/hr, ug/cc, and microparticles/cc using the proportionality constant derived to convert output voltage to units of density.

4.2.1 Algorithm

Below can be found the algorithm followed by the LabVIEW application's calibration function, along with actions that are taken by the operator. It should be noted that the LabVIEW program prompts each step of the calibration and has safety measures in effect that prevent most incorrect settings or inactivity that might occur by the user.

1. **Set user-controlled operating parameters.** Set lock-in amplifier gain (LIA_{GAIN}) and low-pass filter gain (LPF_{GAIN}) to be 100 and 1, respectively. If data acquisition is operating at the default frequency of 10 Hz, set R-C time constant to be 0.03 seconds to ensure that no components of the signal are missed.
2. **Measure the overall DC offset voltage caused by various circuit offset voltages, V_z .** Turn off the laser beam and set the APD bias voltage to be 0 V by shorting the leads together and connecting them to the ground node of the

high-voltage power supply. Acquire the output voltage of the sensor for a period of 60 seconds and take the time average via the following equation, where ‘i’ is the sample number and ‘V_i’ is the ith sample of raw output voltage from the ADS. This offset voltage represents no data of the density signal and will be subtracted from all further measurements.

$$V_Z = \frac{1}{600} \sum_{i=1}^{600} V_i \quad (4)$$

3. **Measure the offset voltage caused by background light sources at an APD gain of 10, V₁.** Turn off the laser beam and set the APD bias voltage to be 134 V, which results in an internal gain of 10 A/A. Acquire the output voltage of the sensor for a period of 60 seconds then take the time average via the following equation. This value will be used in calculating the gain of the APD at a varying operating voltage, where V_i is the ith sample of raw output voltage.

$$V_{AVG} = \frac{1}{600} \sum_{i=1}^{600} \frac{V_i - V_Z}{LIA_{GAIN} * LPF_{GAIN}} \quad (5)$$

4. **Measure the offset voltage caused by the combination of background light and stray laser beam scattering at an APD gain of 10, V₂.** Turn on the laser beam and leave the APD bias voltage steady at the same 134 V. Acquire the output voltage of the sensor for a period of 60 seconds then take the time average via Equation 5. This value will also be used in calculating the gain of the APD at operating bias voltage.

5. **Measure the offset voltage caused by the combination of background light and stray laser beam scattering at an APD gain of 'G', V_3 .** Leave the laser beam turned on and adjust the APD bias voltage to be at the desired operating voltage. For a gain of close to 100 A/A, the recommended bias voltage is 154 V. Acquire the output voltage of the sensor for a period of 60 seconds then take the time average via Equation 5. This value will be used for both calculating the APD gain at the operating bias voltage and subtracting the offsets caused by background and stray laser beam light from the data taken during an experiment run, to more accurately calculate the density data.

6. **Measure the offset voltage caused by background light sources at an APD gain of 'G', V_4 .** Turn off the laser beam and allow the APD bias voltage to remain at its current magnitude (154 V for a gain of 100 A/A). Acquire the output voltage of the sensor for a period of 60 seconds then take the time average via Equation 5. This value will be used to calculate the APD gain at the operating bias voltage.

7. **Calculate the APD gain, G.** Use the previously measured voltages to calculate the gain of the APD at the current bias voltage, G, using Equation 6. Note that the zero-offset voltage, V_z , has been accounted for in the previous measurements and is not required in the present calculation.

$$G = 10 * \frac{V_3 - V_4}{V_2 - V_1} \quad (6)$$

8. **Determine the normalized sensor output voltage at each sample, V_N .** Now that the offset voltage caused by background light and stray laser beam photons present in the raw output is known, it is possible to determine the normalized sensor voltage that is generated by the actual aerosol density signal, where V_i is the i^{th} sample of raw voltage from the sensor and V_N is the instantaneous output voltage independent of known offsets.

$$V_N = V_i - (V_3 * LIA_{GAIN} * LPF_{GAIN}) \quad (7)$$

9. **Perform a 30-minute test run to calibrate the sensor by measuring the amount of particulate mass that has passed through the sensor to calculate the proportionality constant that converts between output voltage and units of density, α .** Turn on the LAMA feed system at a typical feed density and allow the system 1-2 minutes for the flow to stabilize as much as possible. After weighing the mass of a HEPA filter, M_1 , and recording the measurement, place it at the immediate exit of the aerosol flow box to capture all particulate that passes through the sensor. Run the sensor at this constant feed level for 30 minutes while allowing software to record the output voltage at a rate of 10 samples per second. At the end of this calibration run, immediately stop recording output voltage data and measure the new mass of the HEPA filter, M_2 , to determine ΔM . Now, the proportionality constant, α , can be calculated by the following equation based off the work from Gleason [1], where ΔM is the difference in measured mass between the beginning and end of the calibration, G is the measured APD internal gain, Q is the total aerosol flow in units of cubic centimeters per minute (typically 200

sccm), Δt is the time gap between samples (0.1 seconds when sampling at 10 Hz), and V_i is the i^{th} sample of raw output voltage from the sensor.

$$\alpha = \frac{60 * \Delta M * G}{Q * \Delta t * \sum_{i=1}^{18k} \left(\frac{V_i - V_Z}{LIA_{Gain} * LPF_{Gain}} - V_3 \right)} \quad (8)$$

10. Finally, the aerosol density, ρ , can be determined from any further measurements of the raw output voltage. Now that all the internal circuit and component parameters are known, α can be used to calculate the instantaneous aerosol density in units of micrograms per cubic centimeter using Equation 9 and milligrams per hour using Equation 10, where V_0 is the raw sensor output voltage and ρ is aerosol density. To calculate the aerosol density in units of microparticles/cc, it is necessary to provide the software with the mean microparticle diameter for the powder chemistry being used. By using the typical microparticle diameter of 1.5 μm for the silver powder often used in the LAMA, it can be determined that 1 $\mu\text{g}/\text{cc}$ corresponds to an average of 50,000 microparticles/cc as exemplified in Equation 11.

$$\rho \left[\frac{\mu\text{g}}{\text{cc}} \right] = \frac{\alpha}{G} * \left(\frac{V_0 - V_Z}{LIA_{Gain} * LPF_{Gain}} - V_3 \right) \quad (9)$$

$$\rho \left[\frac{\mu\text{g}}{\text{hr}} \right] = \frac{\alpha * Q * 60}{G * 1000} * \left(\frac{V_0 - V_Z}{LIA_{Gain} * LPF_{Gain}} - V_3 \right) \quad (10)$$

$$\rho \left[\frac{\text{particles}}{\text{cc}} \right] = \frac{\alpha * 50,000}{G} * \left(\frac{V_0 - V_Z}{LIA_{Gain} * LPF_{Gain}} - V_3 \right) \quad (11)$$

4.3 TEST PLAN

A test plan has been created for the new version of the ADS to verify that it meets the requirements that will be demanded of it while installed in the LAMA system permanently. Several specific capabilities are important to work correctly in order to be able to consider the improvement project a success. Firstly, it is critical that the sensor be able to detect the aerosol flow at very low density levels, as recent experimentation has been in progress using the LAMA that requires extremely low feed rates. Though a typical experiment with the LAMA system is around 3-5 minutes in length, there are often periods of time that multiple experiments will be completed consecutively in a single afternoon; it is necessary that the sensitivity of the sensor remain stable between calibrations to maintain confidence in the accuracy of the density data being recorded. It is also useful to verify that the sensor performs under both abnormally low and high density levels, since it is impossible to be certain what types of experiments will arise for the LAMA in the future. Finally, it is necessary to test the sensor's response to a large adjustment in aerosol density during run-time to ensure that it is able to handle the impulse-like nature of the sudden increase or decrease in output voltage without causing ringing or unexpected signal loss or saturation.

4.3.1 Lowest Detectable Density

The first test that will be performed on the updated version of the ADS is determining the lowest detectable density that the sensor can detect reliably. Using the feeder proportioning valve, the density will be lowered drastically until it is very near zero and the gain of the system will be increased to the maximum possible. The signal will be monitored to determine at what point the signal no longer represents the density but rather has entered into noise variations of the sensor that is present even with no flow.

4.3.2 Sensitivity Stability

Another test that will be performed on the ADS is to ascertain that it maintains sensitivity stability over a long period of time. Though it is impossible to state absolutely that the stability does not vary slightly during an experiment due to minute bias voltage variation, electronic component changes due to temperature variations, or other uncontrollable environmental variables, it is possible to determine whether significant dust accumulation on the optical windows of the aerosol flow box has occurred. An initial calibration will be performed on the sensor to determine the unamplified output voltage corresponding to the combination of background environmental light and stray laser beam scattering with no aerosol flow through the unit. Next, an aerosol flow of typical density will pass through the system for a long period of time while adjusting no controllable parameters of the sensor. Finally, a second calibration will be performed to determine if there has been any significant change in the voltage resulting from the same background sources; if there is significant change, then it is likely that dusting has occurred on the windows and affected the sensitivity of the sensor.

4.3.3 Low Density Data Quality

An experiment will be run on the LAMA system using a moderately low density to determine the stability and accuracy of the ADS at low density levels. Over a short period of time, the density will visually be estimated to be lower than the typical level by observing the activity of the powder feeder with a member of the research group who is experienced in making such observations.

4.3.4 Average and High Density Data Quality

Similarly, another experiment will occur using the new ADS while running both average and high density levels through the sensor to determine the response of the system. It is important to confirm that the sensor reports reasonable data throughout a range of density levels in the event a design flaw should become apparent due to an unforeseen characteristic of the flow or the sensor itself.

4.3.5 Run-Time Density Adjustment Response

Finally, an experiment will be run during which the operator will cause a sudden and dramatic change in the aerosol density level, both as an increase and as a decrease. The data will be observed to determine that the sensor is able to maintain stability when made subject to an impulse change in input. Additionally, since the operator will certainly be making small adjustments to the aerosol density level during the course of a typical experiment, it is necessary to know if there is a limitation to the speed of change that the sensor is capable of capturing.

Chapter 5: Experimental Results

This chapter discusses the experimental data resulting from completion of the test plan as described in Chapter 4. The quality of the data from the various flow configurations are analyzed and discussed to determine how effective the ADS is at real-time monitoring of the aerosol density used in the LAMA system.

5.1 DATA ANALYSIS

Several experimental tests were run using the new aerosol density sensor installed in the LAMA system. Very low, low, average, and high density levels were used to observe the response and reliability of the ADS under drastically different LAMA configurations. Sanity checks were performed on all data obtained by the sensor to verify proper hardware and software functionality and repeatability. All data values displayed in this section are logged from the custom ADS LabVIEW application and taken from the .xls spreadsheet that was automatically written by the data acquisition function of the software. Plots are created in Microsoft Excel using the raw output data with no further processing.

5.1.1 Lowest Detectable Density

Firstly, an experiment was run to determine the lowest density that the ADS is able to detect. To do this, the proportioning valve that controls the amount of gas that flows through the powder feeder was completely opened in order to decrease the density level to the minimum possible. Simultaneously, all adjustable gain in the system was set to the maximum available. After allowing the flow to stabilize for a period of five minutes, the ADS was used to acquire density level data and the results are shown in the plot below. To ensure that the signal is actually representing a very low density rather than noise around zero, the flow through the system was then completely turned off so that the only remaining signal is the noise. Since this no-flow signal is indeed of a magnitude below that of the minimum achievable density level, it can confidently be claimed that the sensor is able to measure density levels down to the minimum achievable using the current LAMA configuration. By effectively zooming in on the section of data enclosed by the shaded rectangle in Figure 22, it can more easily be concluded that the

density can be measured down to a minimum of approximately 0.15 mg/hr. If the density were to be lowered further than this level, it would begin to merge into the zero-flow signal, which is effectively noise.

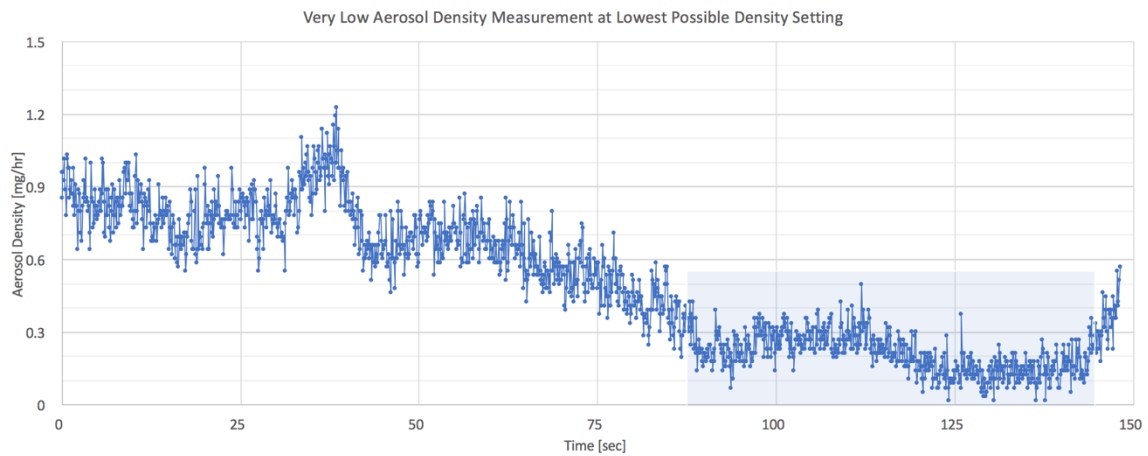


Figure 22: Data Plot of ADS Output in Units of mg/hr for Lowest Possible Density Through the Sensor

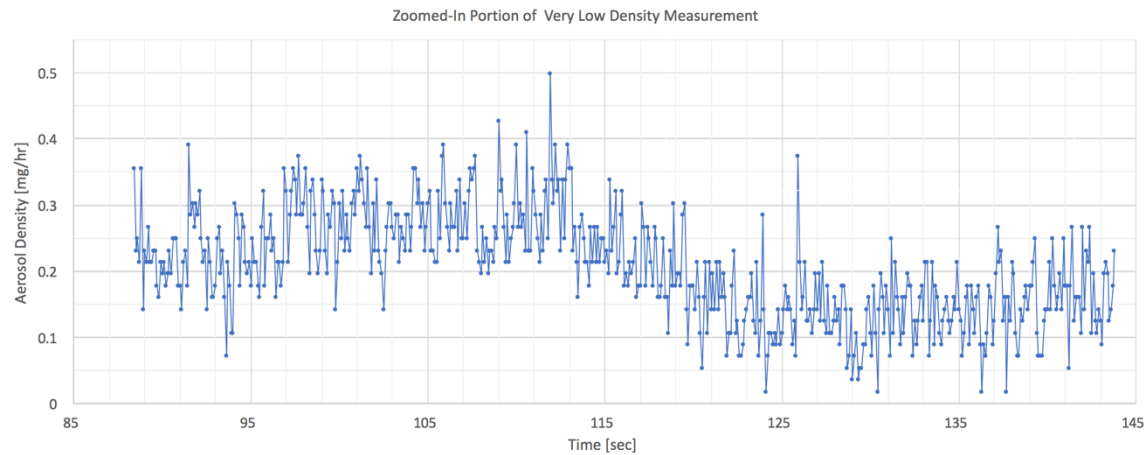


Figure 23: Zoomed-In Portion of Data Plot of ADS Output in Units of mg/hr for Lowest Possible Density Through Sensor

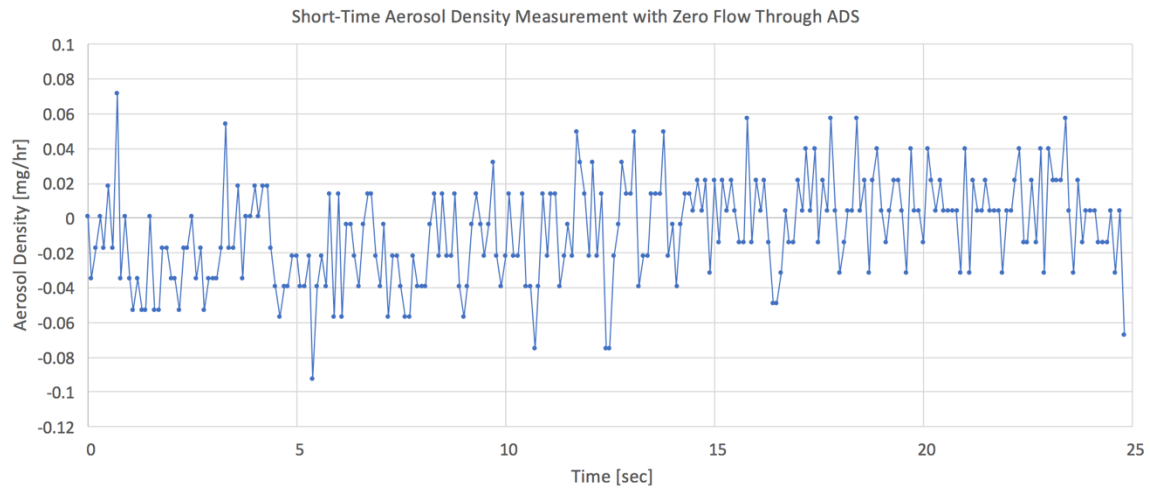


Figure 24: Data Plot of ADS Output in Units of mg/hr for Zero Aerosol Flow through the Sensor

5.1.2 Sensitivity Stability

To perform the sensitivity stability verification test on the new ADS, it was necessary to perform several partial calibrations over a long period of time. An initial calibration was performed when the sensor was first powered on with an operating bias voltage of 146 V. The output voltage of the ADS corresponding to the signal created by the combination of background light and stray laser beam scattering incident upon the APD, is recorded with zero aerosol flow through the sensor. Next, the helium flow in the LAMA system was turned on and a flow containing a typical level of aerosol density was allowed to pass through the sensor while turned on. It is crucial to maintain no change in any controllable physical or electronic circuit parameters or configurations throughout this test, as minute changes by the user would cause the data to be inaccurate. After one hour of constant flow, the density level of the aerosol is turned as low as possible to flush the majority of the existing particulate out of the sensor and into the rest of the LAMA

system. Finally, the aerosol flow was stopped completely and the sensor was left to rest for 15 minutes to allow any final particulate still inside the sensor to settle or evacuate. A second calibration was run while adjusting no parameters of the ADS and the same output voltage was recorded. This process was performed a total of three consecutive times in an attempt to obtain enough data points to form a trend of the transmittance of the optical windows. Though there appears to be a gradual downward trend in the offset voltage throughout the course of the calibrations, the data suggest that no significant amount of accumulation has occurred by the particulate on the surface of the optical windows. Though there is variation in the average offset voltage throughout the calibrations, each falls within the variation of the first calibration run. These small variations, both in the positive and negative direction, are likely caused by small variations in the APD bias voltage, electronic component variations, and noise in the analog-to-digital converter present in the DAQ unit. Below can be seen a plot of the output voltage captured during the 60-second data acquisition that was used to find the average offset voltage corresponding to the background and beam scattering present during the calibration as well as the trend of the V_3 average output voltage values throughout the multiple calibrations.

Time [hours]	V_3 [mV]
0	2.46408
1.25	2.46443
2.5	2.46389
3.75	2.46376
5	2.46414

Table 1: Sensitivity Stability due to Window Transmission Data Record

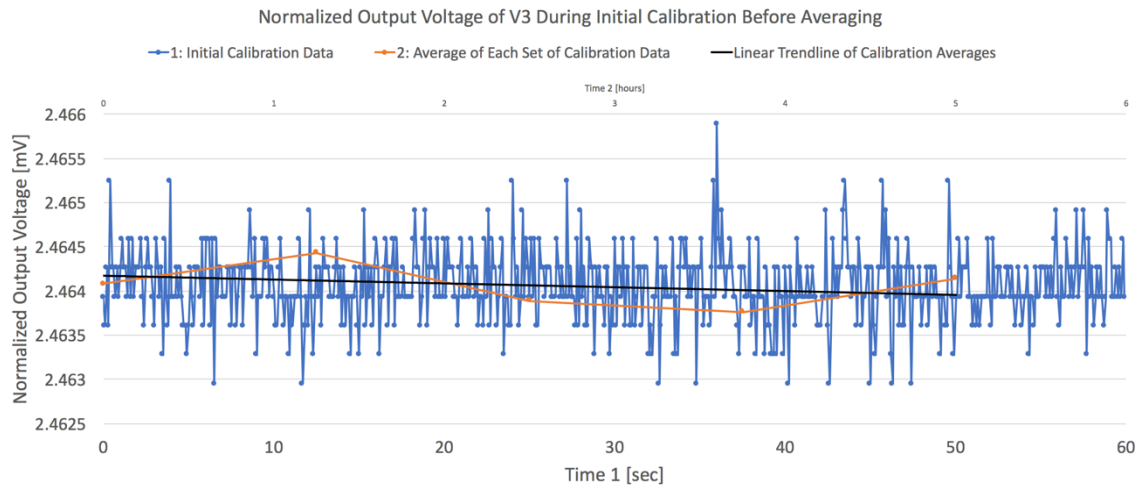


Figure 25: 1) Data Plot of ADS Output at 10 Hz representing background and laser scattering offset voltage, V_3 , 2) Data Plot of time-averaged V_3 across several calibrations, 3) Trend of time-averaged values of V_3 across 5-hour interval

5.1.3 Low Density Data Quality

Another test was performed on the ADS in which it was made subject to an abnormally low aerosol density level of around 5 mg/hr. Over the course of the experiment, the output voltage was monitored to qualitatively determine the quality and consistency of the density data. The following plot displays the resulting data as it was recorded in software without any further processing in Excel other than the creation of the plot itself. Since it is impossible to control the aerosol density to be perfectly constant, some variation in the feed is expected. It can be seen in the data plot that the larger variations in the density measurement are low-frequency in the presence of higher frequency sampling, so is caused by a change in the density level rather than variations by noise in the circuit.

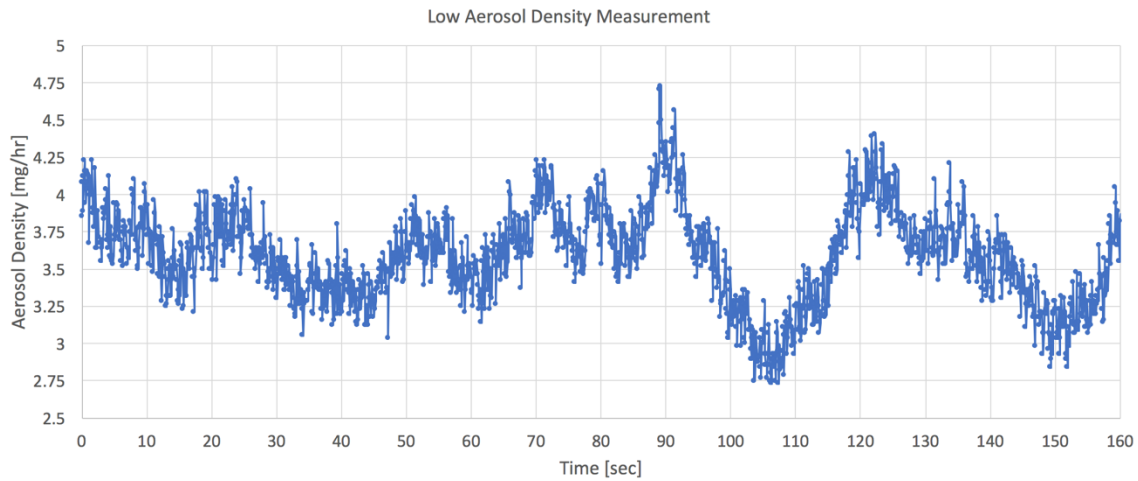


Figure 26: Data Plot of ADS Output in Units of mg/hr for a Low Density Feed

5.1.4 Average and High Density Data Quality

Another set of tests was performed on the sensor while running both a typical and abnormally high level of aerosol density, of around 15 mg/hr and 60 mg/hr, respectively. Similar to before, the data sets were analyzed to ensure that the sensor is able to record the data consistently and with little evidence of significant noise. At the typical density level, there is the expected low-frequency variations in the signal that correspond to changes in the density and is quite steady with few outlying data points. At the high density level, the density is significantly less steady and presents more variation than at lower levels.

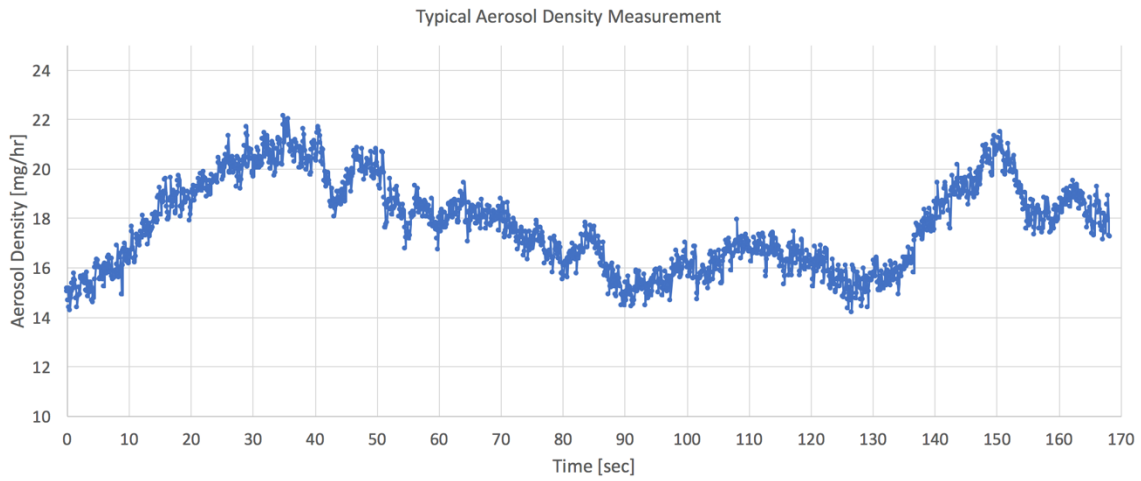


Figure 27: Data Plot of ADS Output in Units of mg/hr for a Typical Density Feed

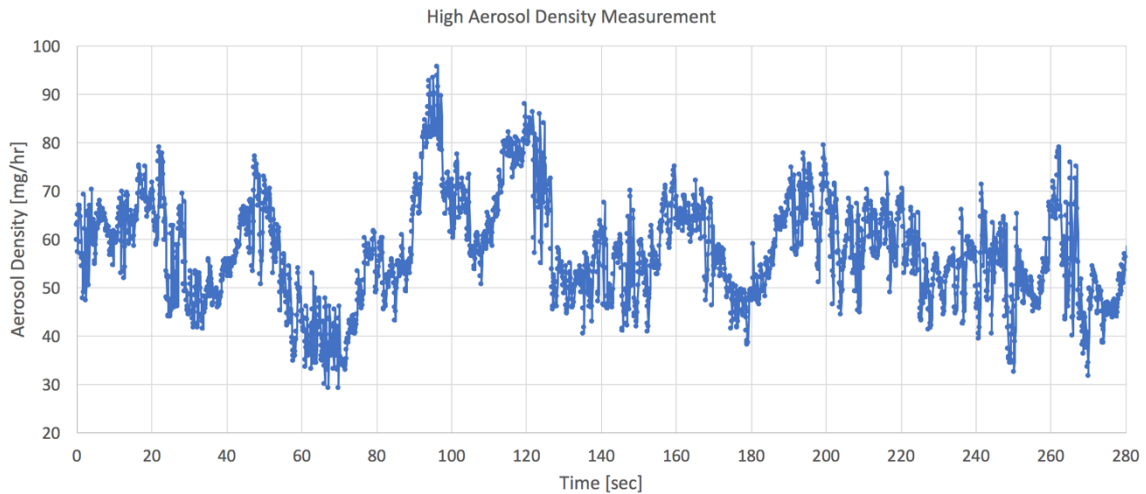


Figure 28: Data Plot of ADS Output in Units of mg/hr for a High Density Feed

5.1.5 Run-Time Density Adjustment Response

The final test experiment performed on the new ADS was to ensure that the sensor is able to respond to impulse changes in the density level while maintaining

stability. First, the density is quickly adjusted from a low level to a very high level, then the opposite is performed. As displayed by the data plot, the sensor is able to record the details of the change since its sampling frequency is sufficiently high, and though the aerosol density took a short amount of time to stabilize at each new level, its output signal remained stable,

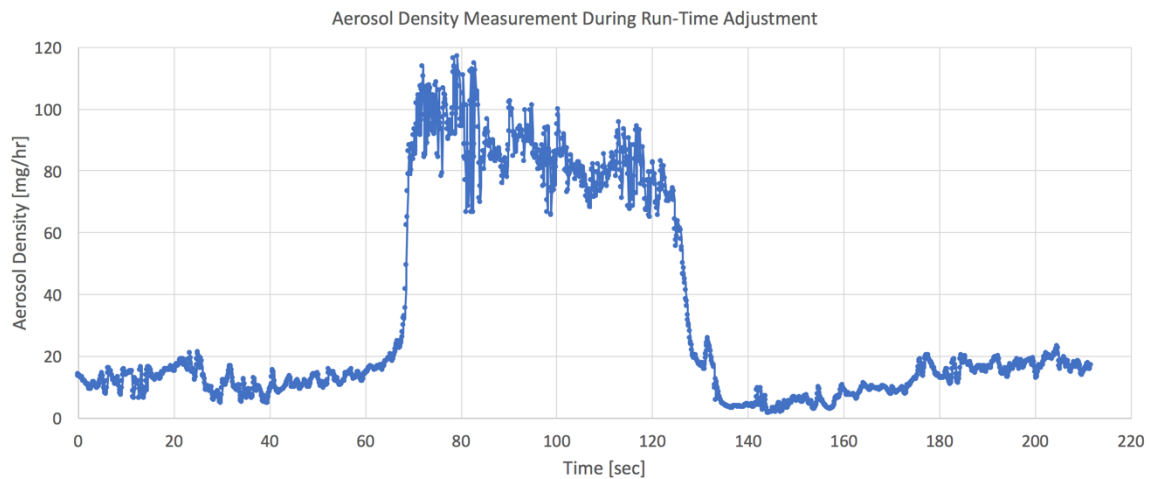


Figure 29: Data Plot of ADS Output in Units of mg/hr During a Run-Time Density Level Adjustment

5.2 EVALUATION OF TEST RESULTS

After completion of all necessary experiments to fulfill the test plan, the results were qualitatively analyzed to determine the overall success of the ADS project. Throughout each of the tests, the sampling frequency of the sensor is at 10 Hz so the density level is able to be monitored very closely. The sensor has been proven to have the capability of detecting extremely low density levels, down to a value of around 0.15 mg/hr. At low to moderate feed densities, the output signal of the sensor maintains

remarkable stability and very low noise. When the feed densities are high, the aerosol feed itself is much less stable and this becomes visible in the ADS signal. At these high levels, the feedstock particles and agglomerates of them do not consistently become suspended in the gas and causes dips and peaks in the signal. Finally, impulsive run-time adjustment of the density level is able to be monitored by the sensor while maintaining sufficient stability.

Chapter 6: Conclusion

This chapter is a conclusion of the test results of the work that was performed in the updating of the aerosol density sensor used in the Laser Ablation of Microparticle Aerosol system by the Nanoparticle Research group at the University of Texas at Austin. Additionally, suggestions for future work is discussed along with any features that were initiated but not completed during the design of the sensor.

6.1 SUMMARY OF RESULTS

Overall, the test results representing the quality of the new design of the ADS suggest that the project has been a success. In the Nanoparticle Research group, the type of experiments that are run on the LAMA system vary in the density level that is used. It has been shown that the new ADS is able to perform, not only under typical conditions, but also with very high or very low levels of aerosol density, with both stability and accuracy. Though it is unknown what type of experiments the future holds for this system, it is clear that the LAMA system will be used with very low density levels; data resulting from the test plan of this sensor proves that it can indeed detect and operate stably at these extremely low density levels. The operator can confidently perform large adjustments to the density level without worry that the sensor will not handle the impulsive input, as has been seen in the data corresponding to large adjustments that the sensor will maintain stability. Additionally, the LabVIEW software added to the sensor system is easy and convenient to use, and provides the group with valuable data that can be used to qualitatively reach conclusions about nanoparticle properties observed on LAMA deposition films.

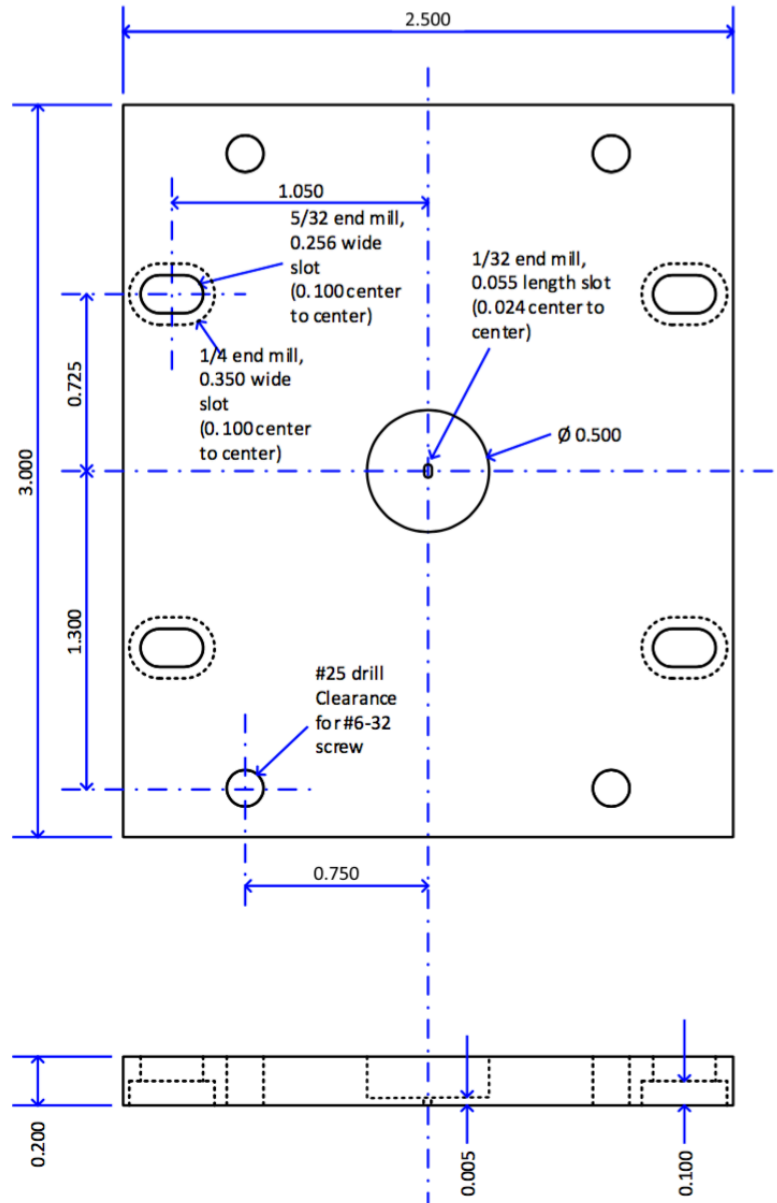
6.2 FUTURE WORK

In the process of implementing the design of the new ADS, time did not allow for one of the planned features to be installed on the sensor. In an attempt to provide autonomous control over the aerosol density level, a motor and motor driver were installed into the ADS system that would have been driven by the LabVIEW control software to automatically maintain the density at a constant level by mechanically adjusting the proportioning valve present upstream of the powder feeder. Due to time constraints and unanticipated difficulties arising from other aspects of the project, the

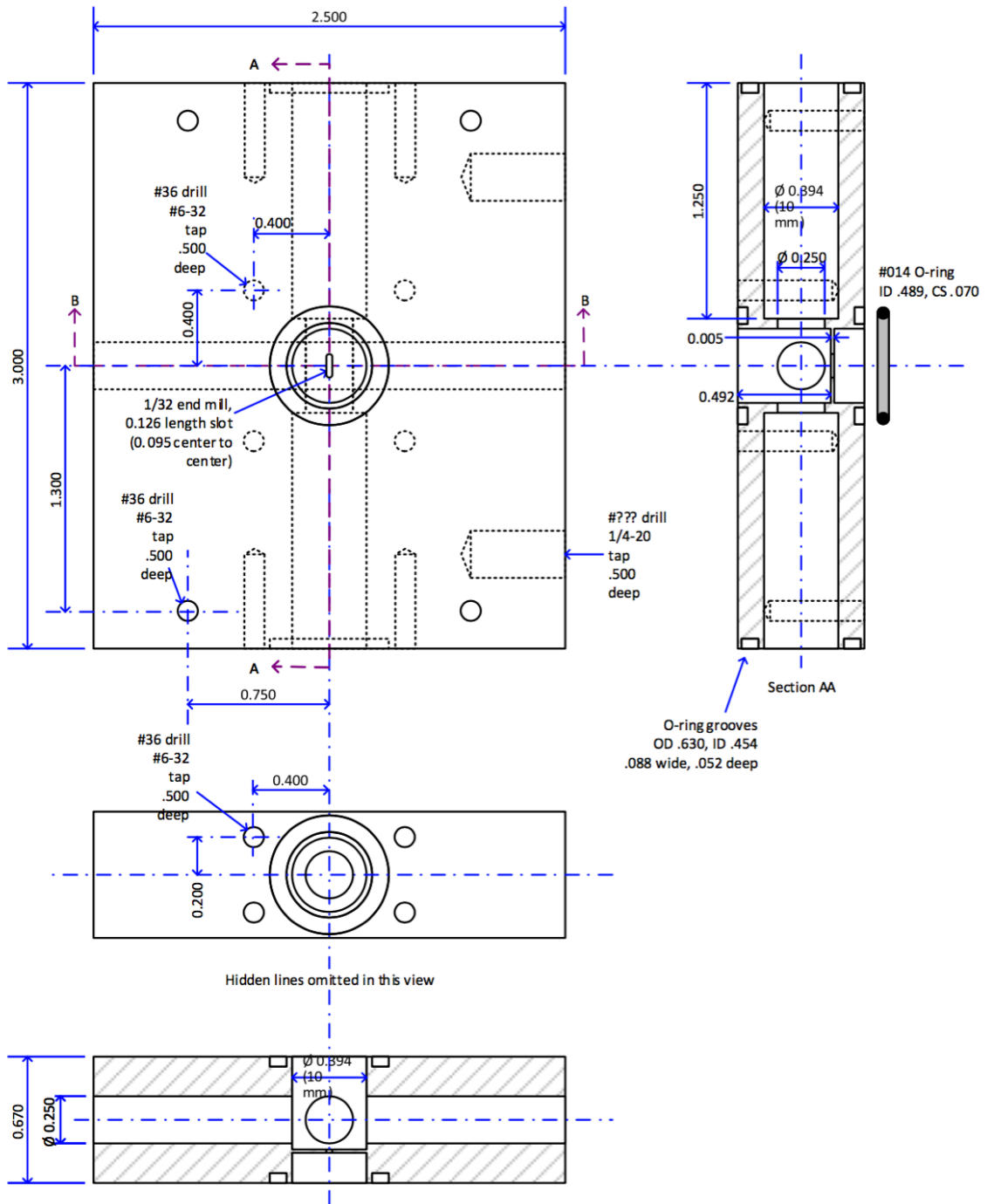
motor and driver were installed into the system but the control software was not fully developed. The NI myDAQ is able to provide an output signal at a sufficient frequency necessary to control the motor driver, but the PID or counter method in the software must still be created. This functionality was intended to be left as future work for the ADS design to provide the operator with a more advanced way to steady the density level.

Appendix A: Mechanical Drawings

Mounting Plate for Sensor Board

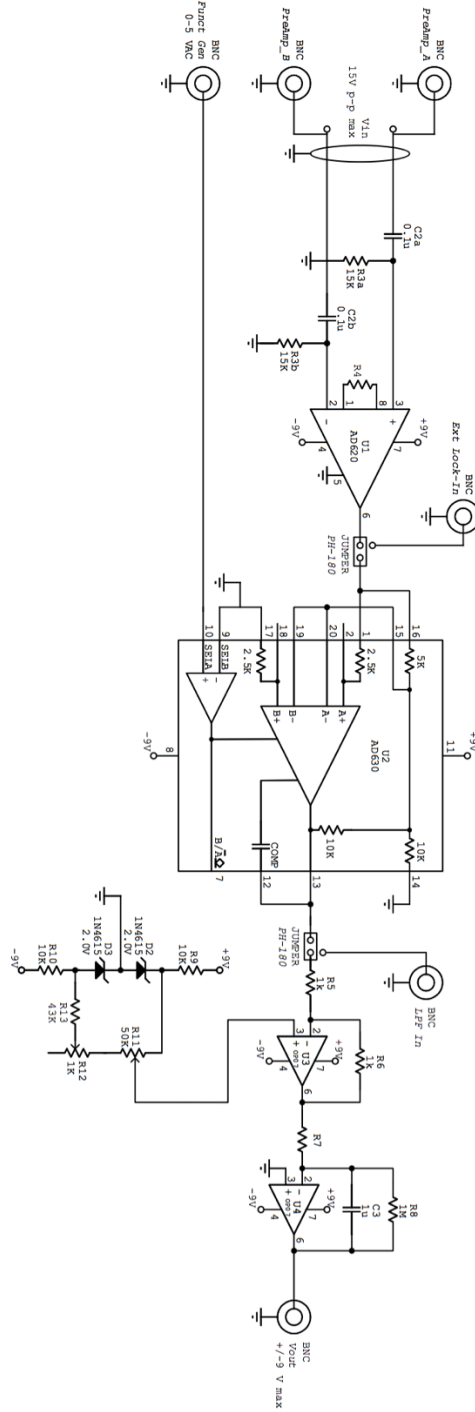


Aerosol Flow Box Cross Cell

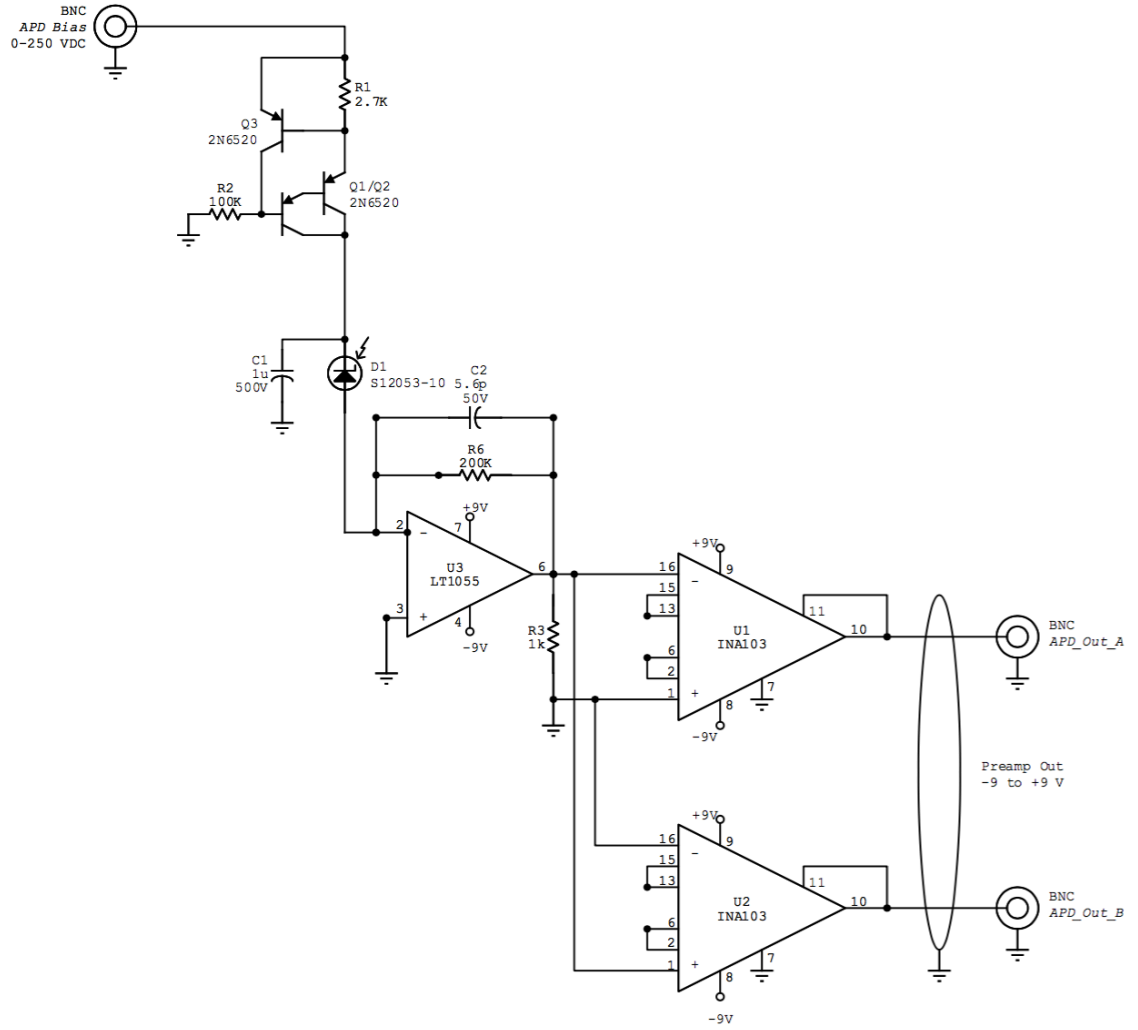


Appendix B: Hardware and Circuit Schematics

Circuit Schematic of Amplifier, Lock-In Amplifier, and Filter Module

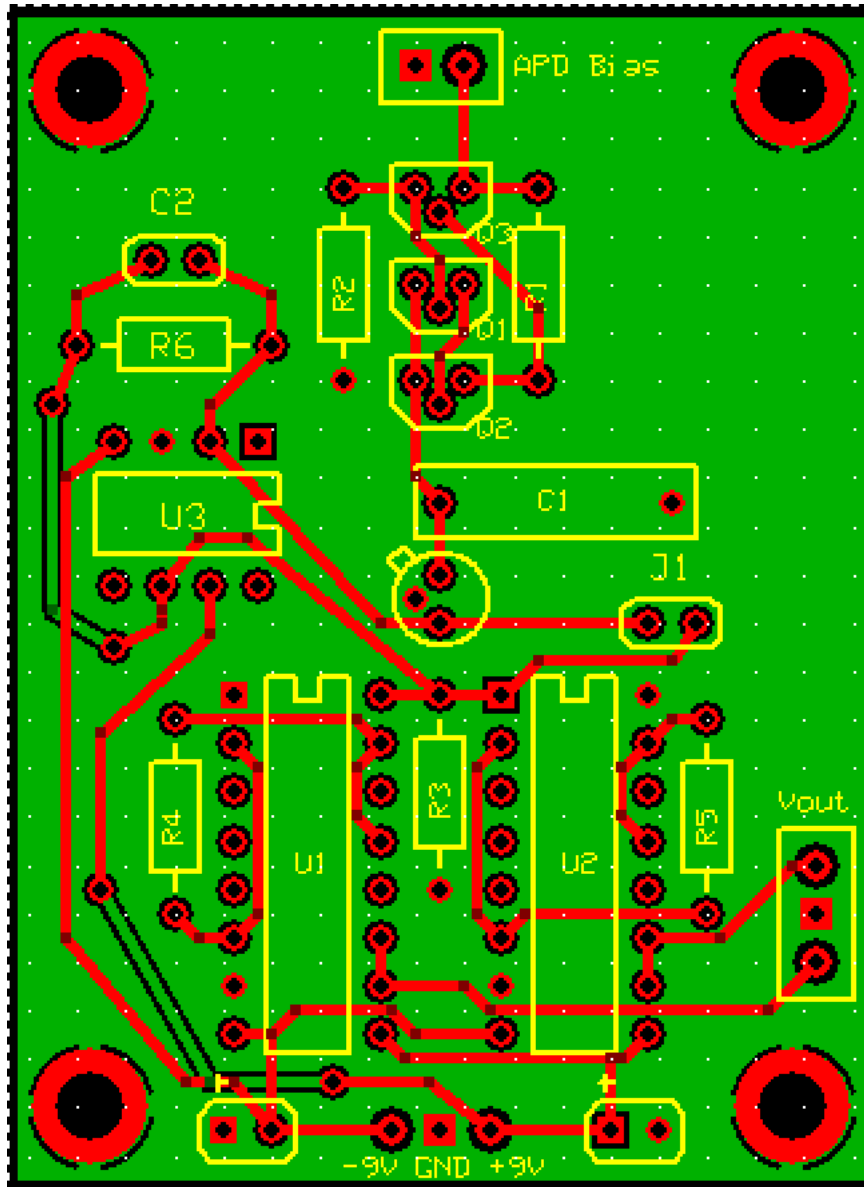


Circuit Schematic of Sensing And Pre-Amplification Module

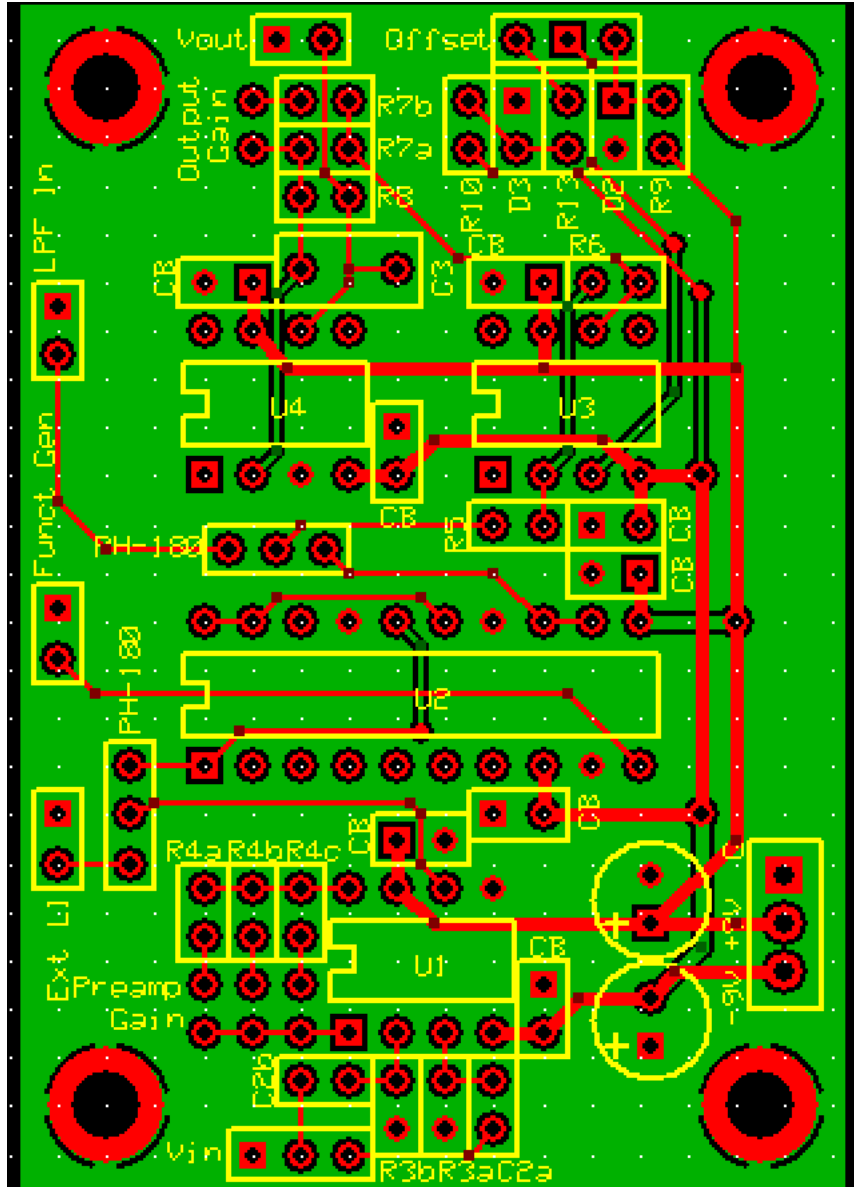


Appendix C: PCB Schematics

Sensing and Pre-Amplifier Circuit PCB

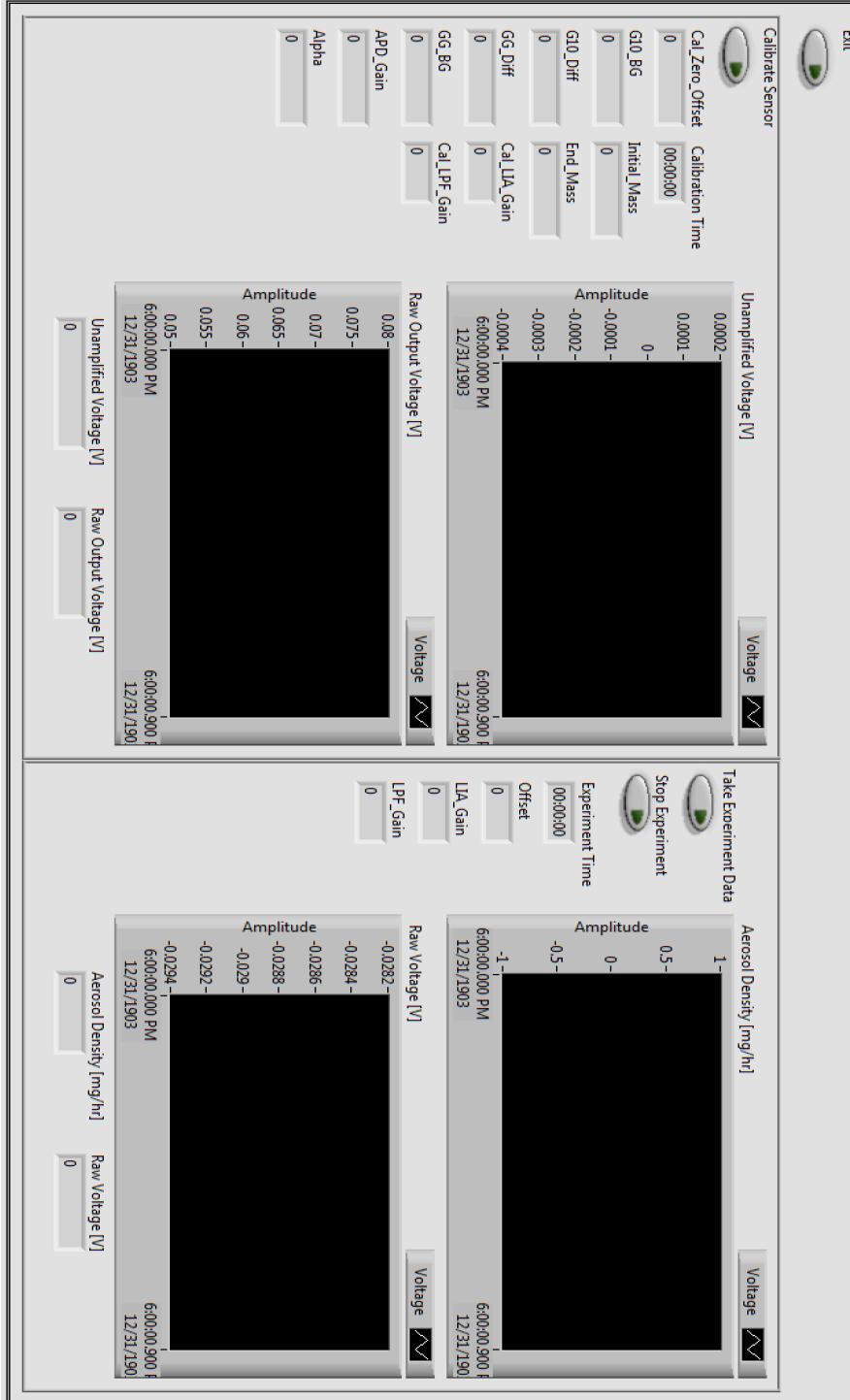


Amplifier, Lock-In Amplifier, and Filter Circuit PCB



Appendix D: Graphical User Interface Images

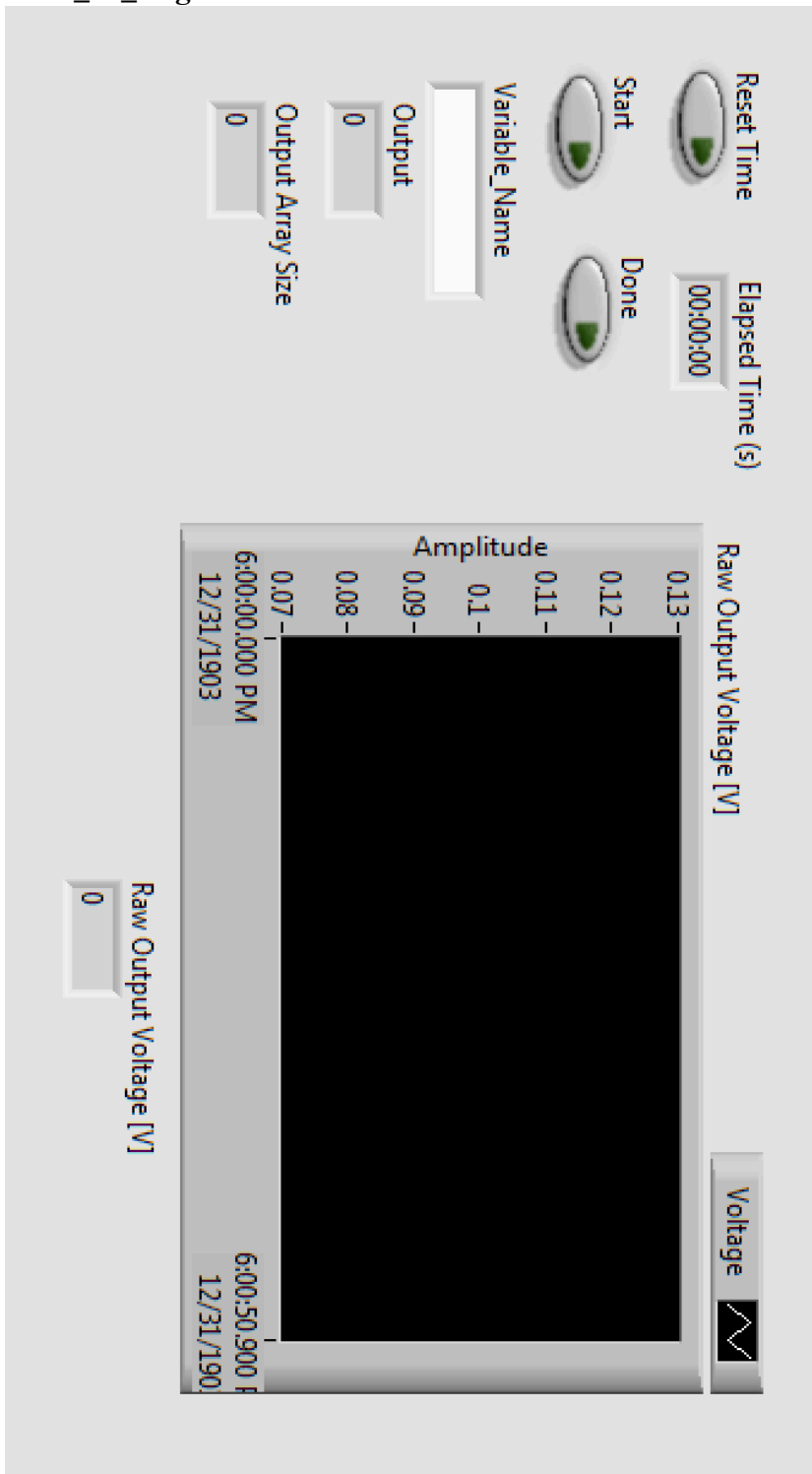
Application Front Panel



Exp_Run SubVI Front Panel



Take_60_Avg SubVI Front Panel



Get_60_Deamp_Avg SubVI Front Panel

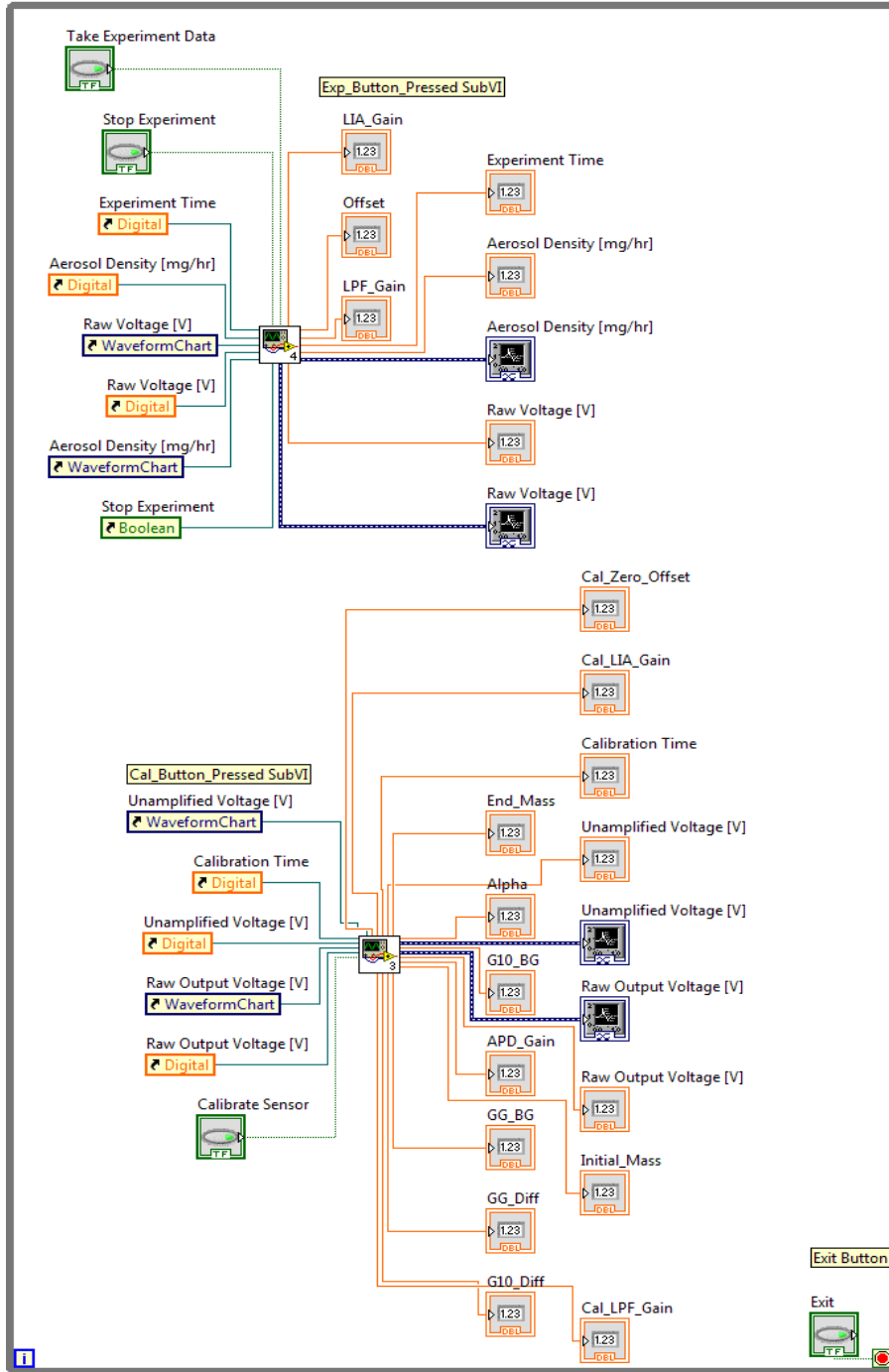
The front panel includes the following controls and displays:

- Control Buttons:** Start, Done, Reset Time, Output (0), output array (0), Output Array Size (0), and a +/- button.
- Time Displays:** Elapsed Time (s) showing 00:00:00.
- Amplitude Plots:**
 - Offset Adjusted [V]:** Y-axis from -0.02 to 0.08. X-axis shows 6:00:00.000 PM 12/31/1903 and 6:04:33.886 F 12/31/1903.
 - Raw Output Voltage [V]:** Y-axis from -0.02 to 0.08. X-axis shows 6:00:00.000 PM 12/31/1903 and 6:04:33.886 F 12/31/1903.
 - Unamplified Voltage [V]:** Y-axis from -0.0002 to 0.0008. X-axis shows 6:00:00.000 PM 12/31/1903 and 6:04:33.886 F 12/31/1903.
- Input Fields:** Raw Output Voltage [V] and Unamplified Voltage [V] both set to 0.
- Checkboxes:** Voltage checkboxes are present below each plot.

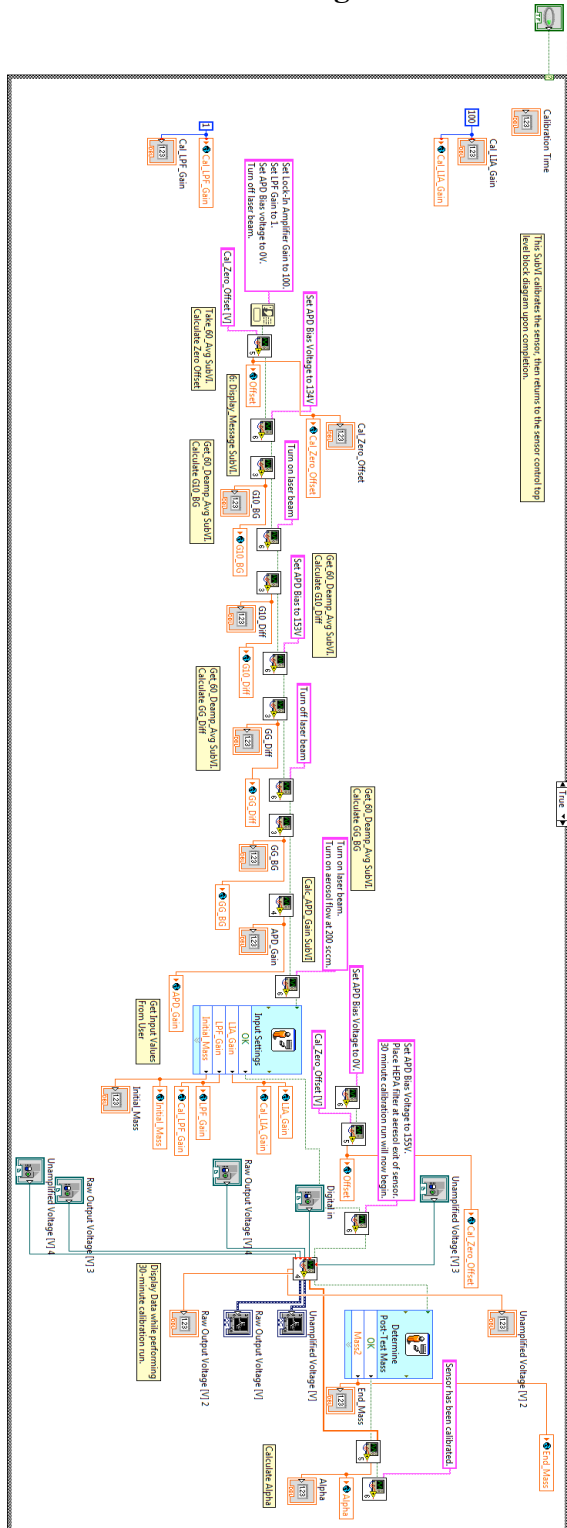
Appendix E: Software Diagrams

Sensor_Control_Top Application Top Level VI, Block Diagram

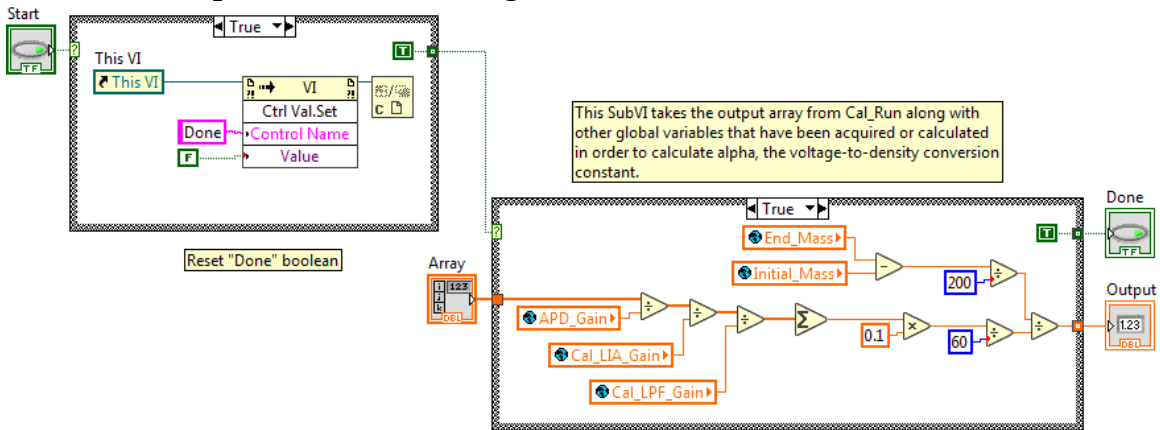
This VI is the top level block diagram. It acts as the base for the state machine.



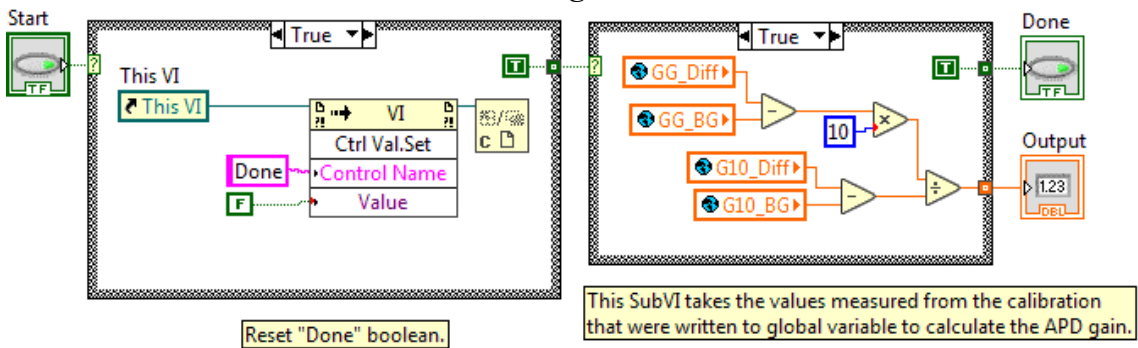
Cal_Button_Pressed SubVI Block Diagram



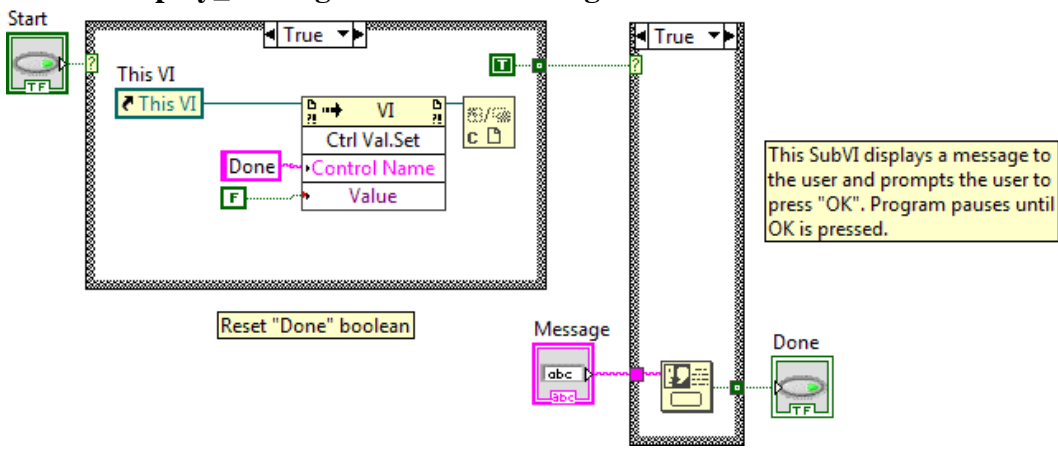
Calc_Alpha SubVI Block Diagram



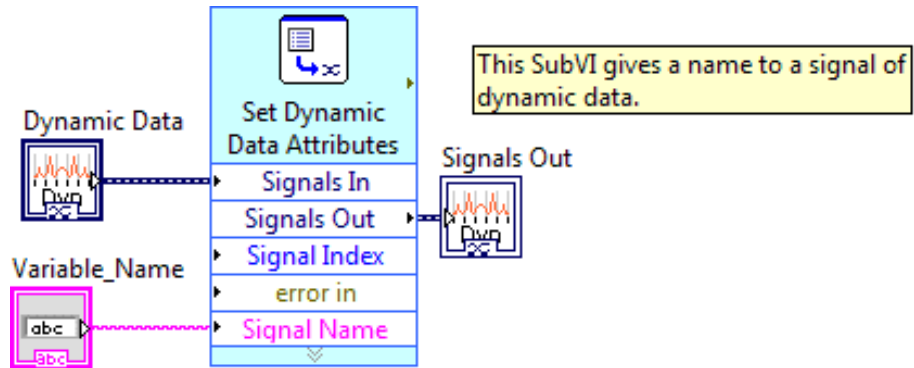
Calc_APD_Gain SubVI Block Diagram



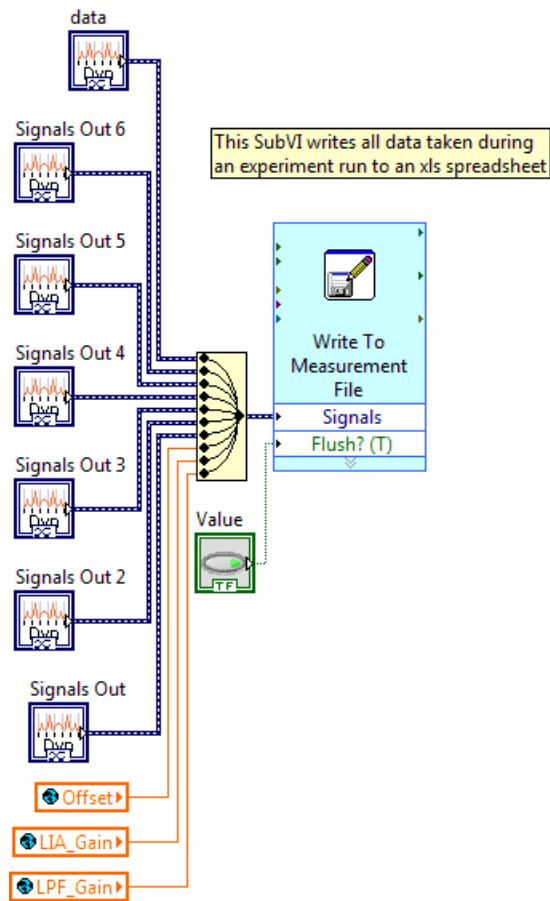
Display_Message SubVI Block Diagram



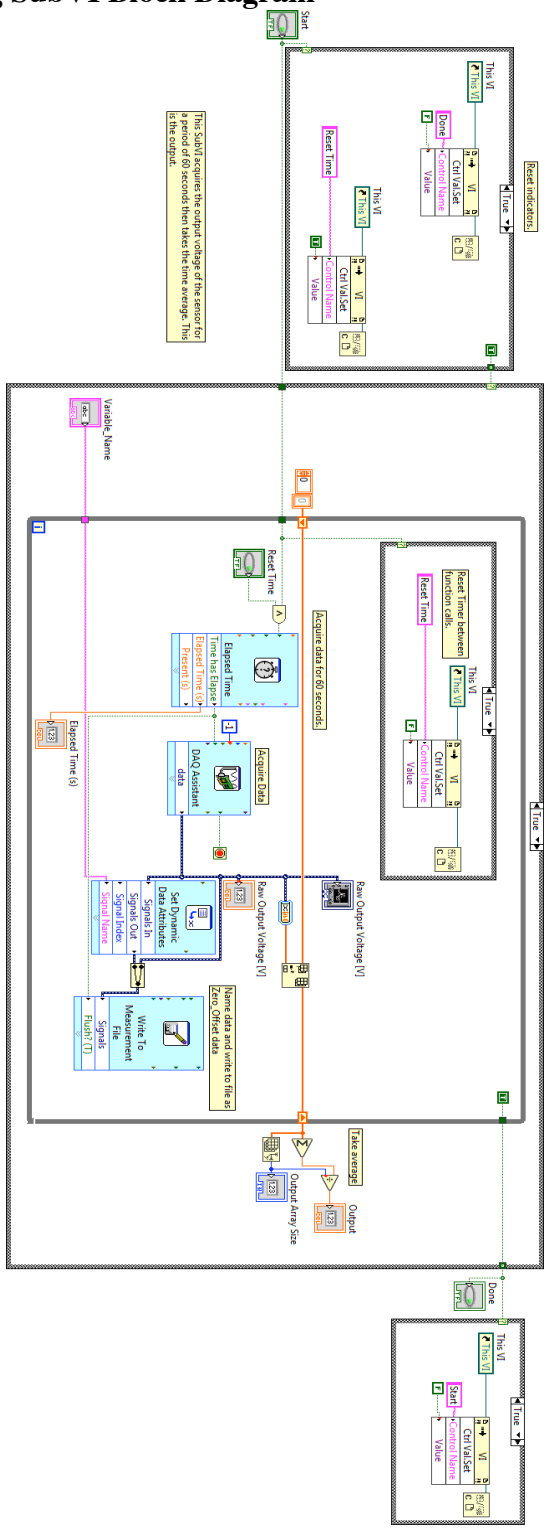
Set_Attributes SubVI Block Diagram



Write_ExpData SubVI Block Diagram

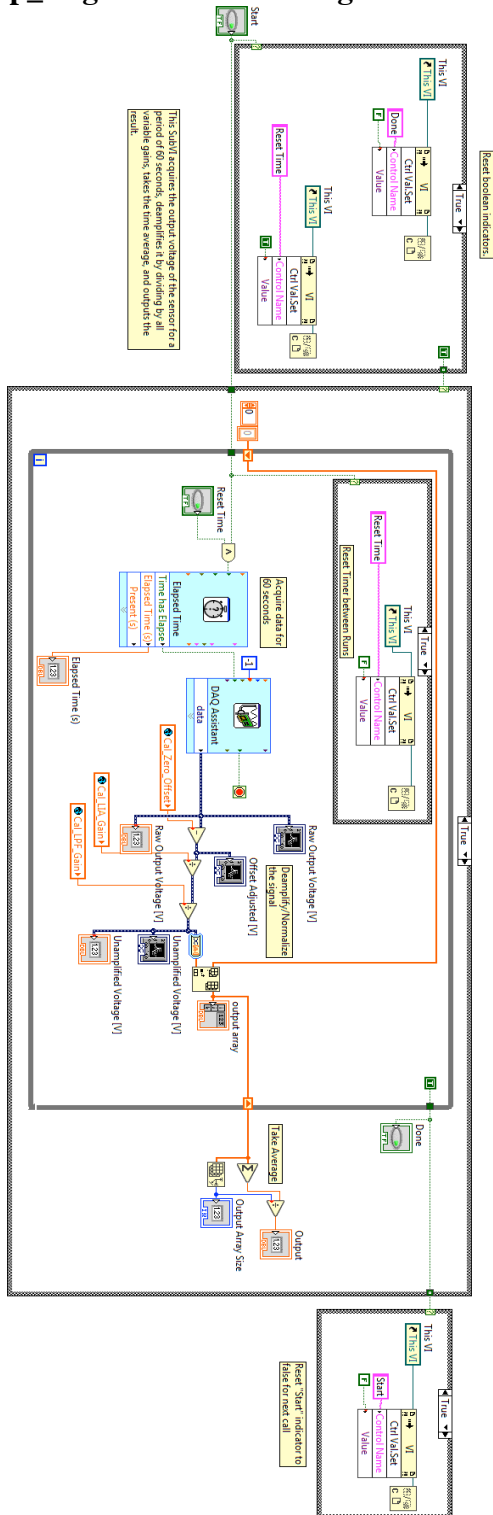


Take_60_Avg SubVI Block Diagram

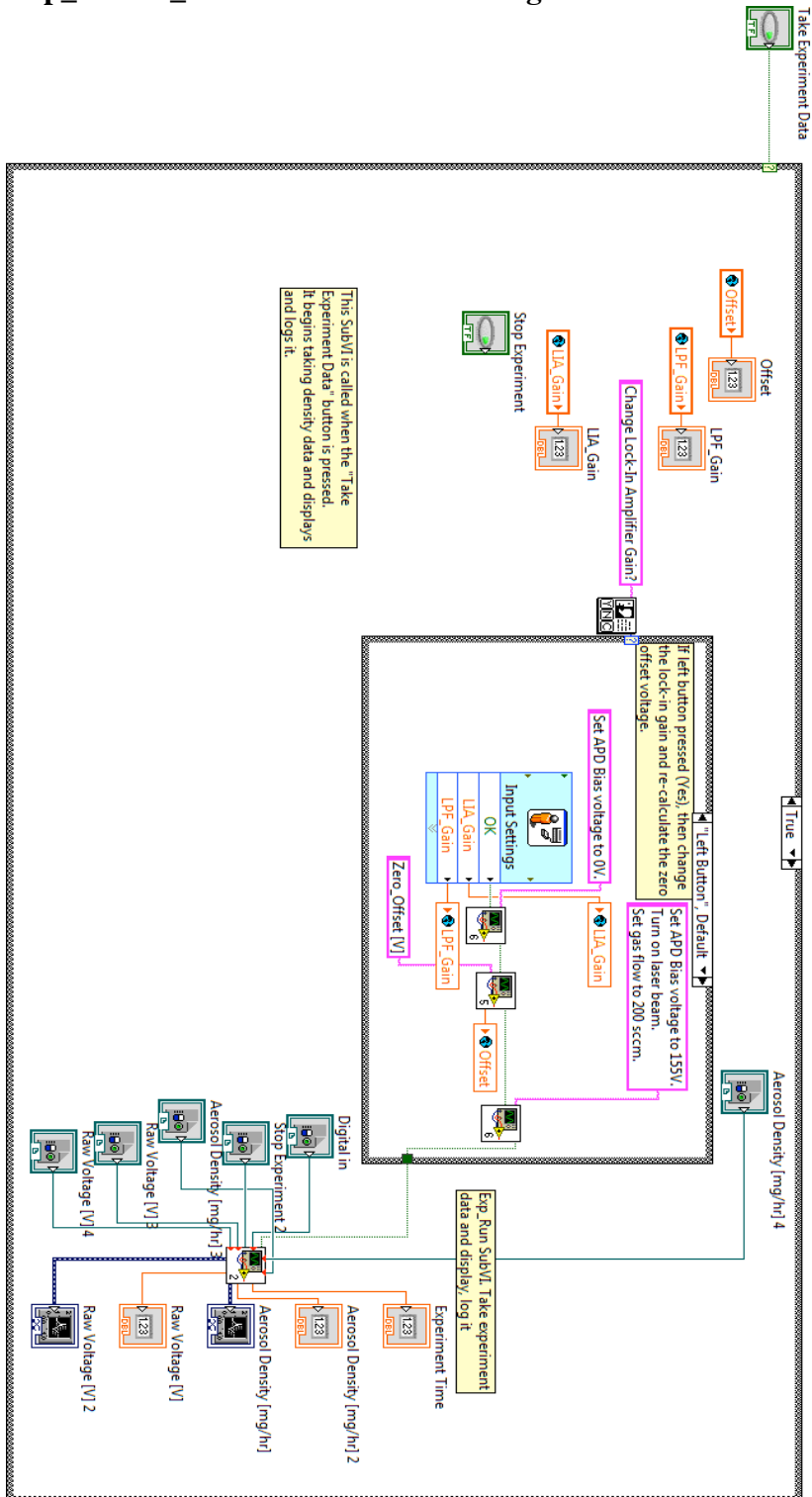


This SubVI acquires the output voltage of the sensor for a period of 60 seconds then takes the time average. This is the output.

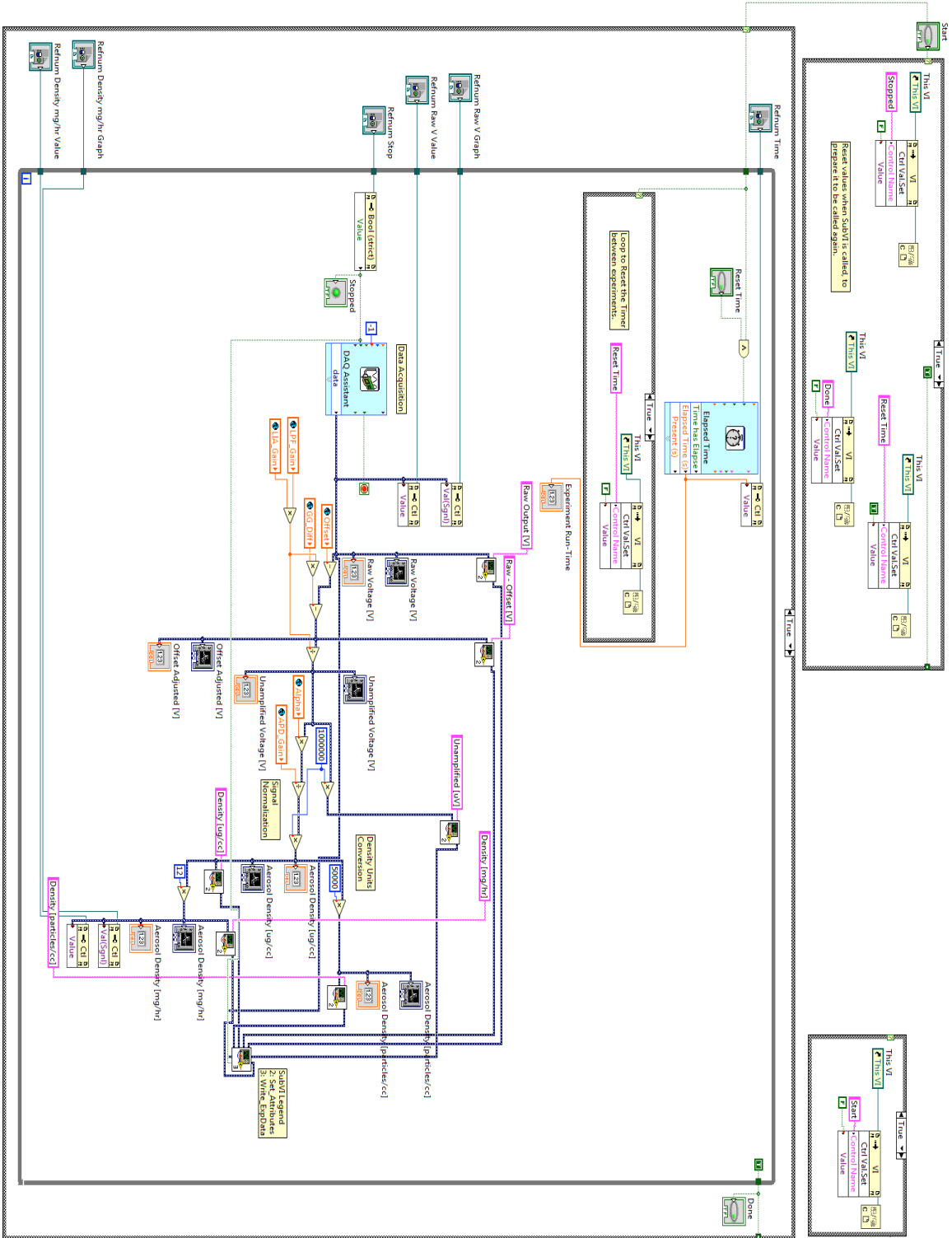
Get_60_Deamp_Avg SubVI Block Diagram



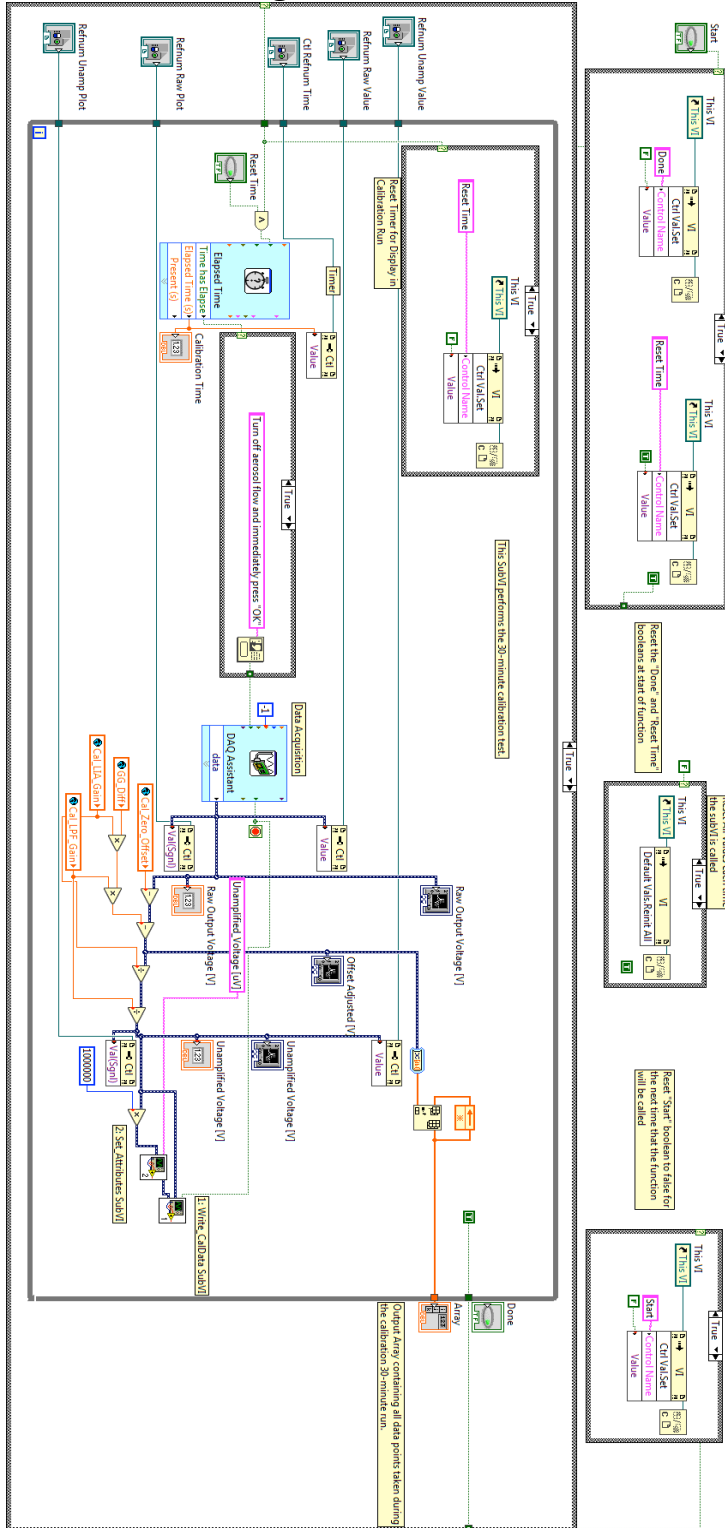
Exp_Button_Pressed SubVI Block Diagram



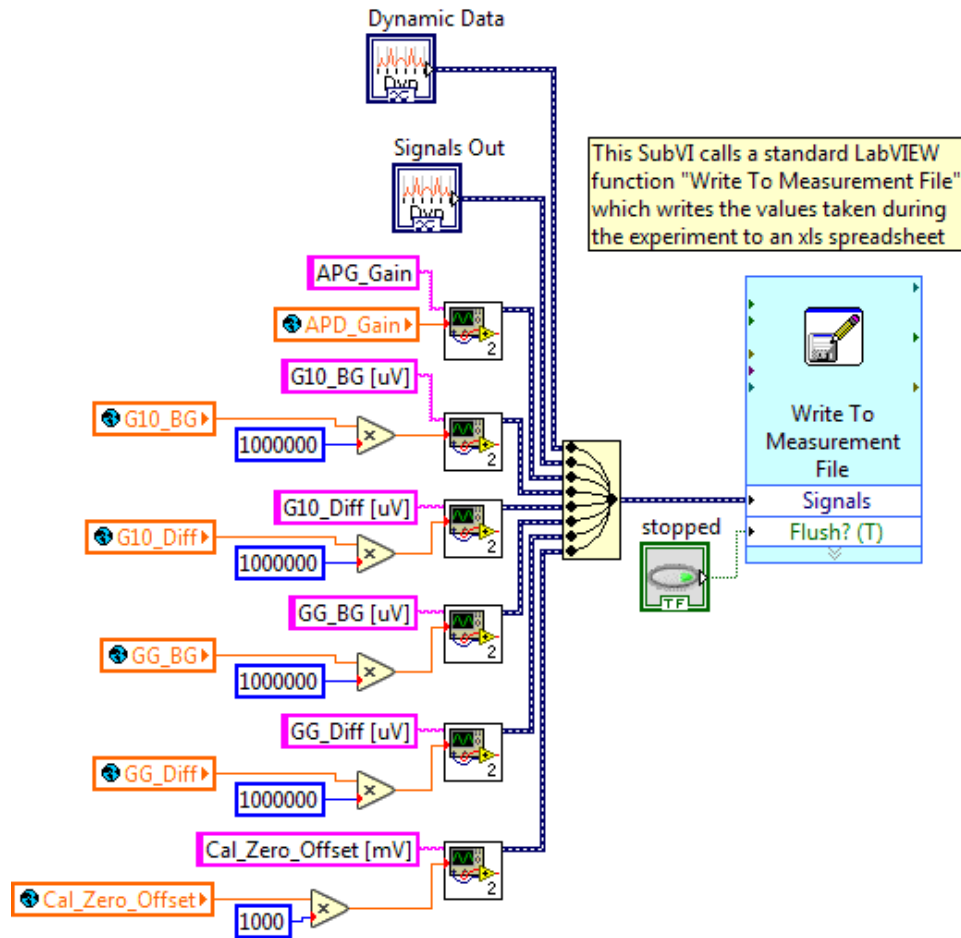
Exp_Run SubVI Block Diagram



Cal_Run SubVI Block Diagram



Write_CalData SubVI Block Diagram



References

- [1] Gleason, K. L. (2011). *Engineering Nanocomposite Polymer Membranes for Olefin/Paraffin Separation* (Doctoral dissertation, The University of Texas at Austin). Retrieved from <https://repositories.lib.utexas.edu/bitstream/handle/2152/ETD-UT-2011-12-4374/GLEASON-DISSERTATION.pdf?sequence=1>
- [2] Keto, J. W. (2006, April 11). Laser spectroscopy and nanoparticle research at the University of Texas in Austin. Retrieved from <https://web2.ph.utexas.edu/~laser/>
- [3] Clark, J. and Gunawardena, G. (2017, February 10). The Beer-Lambert Law. Retrieved from https://chem.libretexts.org/Core/Physical_and_Theoretical_Chemistry/Spectroscopy/Electronic_Spectroscopy/Electronic_Spectroscopy_Basics/The_Beer-Lambert_Law
- [4] Pacific Silicon Sensor Incorporated, “Pacific Silicon Sensor Series 8 Data Sheet”, AD800-8-T052-S1 datasheet (2009, December 22)
- [5] Texas Instruments Incorporated. (2000). *Noise Analysis of FET Transimpedance Amplifiers* [PDF file]. Retrieved from www.ti.com/lit/an/sboa060.pdf
- [6] Tenenergy. (2015). Tenenergy TN137 10-Bay 9V Charger. Retrieved from www.tenenergy.com/01137
- [7] Hamamatsu Photonics. (2013). *Short Wavelength Type APD, for 600 nm Band* [PDF file]. Retrieved from www.hamamatsu.com/resources/pdf/ssd/s12053-02_etc_kapd1001e.pdf

- [8] Linear Technology, “Precision, High Speed, JFET Input Operational Amplifiers”, LT1055/LT1056 datasheet (1994).
- [9] Analog Devices, “Low Cost Low Power Instrumentation Amplifier”, AD620 datasheet (2011).
- [10] Analog Devices, “Balanced Modulator/Demodulator”, AD630 datasheet (2016).
- [11] Sengupta, S., Farnham J., & Whitten, J. (2005). *A Simple Low-Cost Lock-In Amplifier for the Laboratory* [PDF file]. Retrieved from pubs.acs.org/doi/abs/10.1021/ed082p1399?guest=true&
- [12] National Instruments. (2015, October 6). Tutorial: state machines. Retrieved from www.ni.com/tutorial/7595/en/

Vita

Daniel Edward Wimmer, son of Randy and Linda Wimmer, was born on November 6, 1990 in Denton, Texas. He attended The University of New Mexico in Albuquerque, NM to achieve a B.S. in Electrical Engineering in May 2015. Upon entrance to the Sandia National Laboratories Critical Skills Master's Program under the National Physical Science Consortium Fellowship, Daniel enrolled in the Cockrell graduate school of engineering at The University of Texas at Austin. He earned an M.S.E. in Electrical and Computer Engineering in May 2017 under the supervision of Dr. Michael F. Becker.

Email: danielewimmer@gmail.com

This thesis was typed by the author.